ARTICLE
Journal of Cellular Biochemistry 114:1987–1996 (2013)
Journal of Cellular Biochemistry

Suppressive Effect of the Histone Deacetylase Inhibitor Suberoylanilide Hydroxamic Acid (SAHA) on Hepatitis C Virus Replication

Ayami Sato,[1] Yoshimasa Saito,[1,2] Kazuo Sugiyama,[2] Noriko Sakasegawa,[1] Toshihide Muramatsu,[1] Shinya Fukuda,[1] Mikiko Yoneya,[1] Masaki Kimura,[1] Hirotoshi Ebinuma,[2] Toshifumi Hibi,[2] Masanori Ikeda,[3] Nobuyuki Kato,[3] and Hidetsugu Saito[1,2*]

[1]*Division of Pharmacotherapeutics, Keio University Faculty of Pharmacy, Tokyo, 1058512, Japan*
[2]*Department of Internal Medicine, Keio University School of Medicine, Tokyo, 1608582, Japan*
[3]*Department of Molecular Biology, Okayama University Graduate School of Medicine and Dentistry, Okayama, 7008558, Japan*

ABSTRACT

The histone deacetylase (HDAC) inhibitor suberoylanilide hydroxamic acid (SAHA) has a clinical promise for treatment of cancer including hepatocellular carcinoma (HCC). To investigate effect of SAHA on hepatitis C virus (HCV) replication, we treated the HCV replicon cell OR6 with SAHA. HCV replication was significantly inhibited by SAHA at concentrations below 1 μM with no cellular toxicity. Another HDAC inhibitor, tricostatin A, also showed reduction of HCV replication. The microarray analysis and quantitative RT-PCR demonstrated up-regulation of *osteopontin* (*OPN*) and down-regulation of *apolipoprotein-A1* (*Apo-A1*) after SAHA treatment. Direct gene induction of *OPN* and knockdown of *Apo-A1* also showed reduction of HCV replication. The liver specific *microRNA-122*, which is involved in HCV replication, was not affected by SAHA treatment. These results suggest that SAHA has suppressive effect on HCV replication through alterations of gene expression such as *OPN* and *Apo-A1* in host cells. Epigenetic treatment with HDAC inhibitors may be a novel therapeutic approach for diseases associated with HCV infection such as chronic hepatitis, liver cirrhosis, and HCC. J. Cell. Biochem. 114: 1987–1996, 2013. © 2013 Wiley Periodicals, Inc.

KEY WORDS: SUBEROYLANILIDE HYDROXAMIC ACID; HEPATITIS C VIRUS; OR6; *MIR-122*; *OSTEOPONTIN*; *APOLIPOPROTEIN-A1*

Hepatitis C virus (HCV) infection is a major worldwide health problem and approximately 170 million people are infected with the virus. Roughly 60–80% of who carry HCV progress to chronic infection, in which liver cirrhosis and hepatocellular carcinoma (HCC) are frequent complications [Lauer and Walker, 2001]. Treatment of HCV infection has been progressed with introduction of protease inhibitors. Although the combination therapy with pegylated interferon (PEG-IFN), ribavirin, and protease inhibitors has shown a higher sustained virological response (SVR) rate, the SVR rate of patients with genotype 1b and a high viral load has not been satisfactory [Ikeda et al., 2006; Ebinuma et al., 2012; Takayama et al., 2011]. Effective drugs without severe side effects are needed for treatment of chronic infection with HCV genotype 1b.

HCV itself cannot replicate or proliferate with its own protein and nucleic acids, and instead relies on various host factors [Tu et al., 1999; Gao et al., 2004; Hamamoto et al., 2005; Okamoto et al., 2006]. It is possible to attenuate viral replication by stimulating some of these host factors [Kaul et al., 2009; Chen et al., 2010; Vaillancourt et al., 2012]; one such possibility involves epigenetic alterations. Epigenetics is an acquired modification of methylation and/or acetylation of chromatin DNA or histone proteins, which regulates downstream gene expression. Epigenetic alterations can be induced by aging, chronic inflammation, or viral infection.

Disclosure Statement: No conflicts of interest exist.
Grant sponsor: The Japan Society for the Promotion of Science (JSPS); Grant sponsor: Grant-in-Aid for Young Scientists A; Grant number: 23680090; Grant sponsor: Grant-in-Aid for Scientific Research C; Grant number: 24590993; Grant sponsor: Keio Gijuku Academic Development Fund; Grant sponsor: Takeda Science Foundation; Grant sponsor: Inaida Foundation.
*Correspondence to: Hidetsugu Saito, MD, PhD, Division of Pharmacotherapeutics, Keio University Faculty of Pharmacy, 1-5-30 Shiba-kohen, Minato-ku, Tokyo 1058512, Japan. E-mail: hsaito@a2.keio.jp
Manuscript Received: 16 August 2012; Manuscript Accepted: 5 March 2013
Accepted manuscript online in Wiley Online Library (wileyonlinelibrary.com): 20 March 2013
DOI 10.1002/jcb.24541 • © 2013 Wiley Periodicals, Inc.

Aberrations in DNA methylation and histone modification may induce inactivation of tumor suppressor genes and play critical roles in the initiation and progression of human cancer [Gal-Yam et al., 2008]. Moreover, a recent study has demonstrated that the liver-specific microRNA (miRNA) *miR-122* binds to the 5′ noncoding region of the HCV genome and facilitates HCV replication [Jopling et al., 2005; Sarasin-Filipowicz et al., 2009]. MiRNAs are small non-coding RNAs that function as endogenous silencers of various target genes and are expressed in a tissue-specific manner. MiRNAs play important roles in cell proliferation, apoptosis, and differentiation [Schickel et al., 2008]. We have recently reported that some miRNAs are regulated by epigenetic alterations such as DNA methylation and histone modification at their CpG island promoters [Saito et al., 2006].

Unlike genetic alterations, which are almost impossible to reverse, epigenetic aberrations are potentially reversible, allowing the malignant cell population to revert to a more normal state [Kurita et al., 2010]. Chromatin-modifying drugs such as DNA methylation inhibitors and histone deacetylase (HDAC) inhibitors have clinical promise for cancer therapy [Yoo and Jones, 2006]. The HDAC inhibitor suberoylanilide hydroxamic acid (SAHA) is emerging as a promising agent for epigenetic therapy of human malignancies including HCC [Butler et al., 2002]. SAHA was recently approved in Japan for the treatment of cutaneous T-cell lymphoma [Watanabe et al., 2010].

In the present study, we investigated the effect of SAHA on HCV RNA replication in the replicon cell OR6, in which genotype 1b full-length HCV RNA replicates and HCV RNA replication can be monitored by luciferase reporter assay [Ikeda et al., 2005]. Here we show that SAHA has a suppressive effect on HCV replication through changes of gene expression in OR6 cells, suggesting that HDAC inhibitors could be promising drugs for diseases associated with chronic HCV infection.

MATERIALS AND METHODS

CELL CULTURE

OR6 cells were cultured in Dulbecco's modified Eagle's medium (DMEM; Gibco) with 4.5 g/L glucose (Gibco) with 10% heat inactivated fetal bovine serum (FBS; BioWest), 1% penicillin-streptomycin solution (Sigma-Aldrich Japan, Tokyo), and 50 mg/ml G-418 (Roche Diagnostics Co.) in 5% CO_2 in humidified air at 37°C as described previously [Nakamura et al., 2008].

SAHA AND TRICHOSTATIN A (TSA) TREATMENT

SAHA (Sigma-Aldrich) and TSA (Sigma-Aldrich) were dissolved in dimethylsulphoxide (DMSO, Sigma-Aldrich) and ethanol, respectively, and added to culture medium. As a control, DMSO or ethanol diluted with culture medium was used.

MTT ASSAY

Cell proliferation was also measured using the MTT Cell Proliferation Assay Kit (Cayman Chemical). OR6 cells were seeded at 1.0×10^4 cells/well in a 96-well plate and cultured for 24 h. SAHA (0.1, 0.5, 1.0, 1.5, 3.0, and 5 μM) was added and the cells were further cultured for 72 h. MTT reagent (10 μM) was added to each well and the plate was the shaken for 1 min and subsequently incubated at 37°C for 3 h. A sample from each well was mixed with 100 μl Crystal Dissolving solution and shaken for 30 min, and the absorption was measured at 570 nm.

CELL NUMBER COUNTING

OR6 cells were seeded at 1.0×10^5 cells/well in a 6-well plate, and 1.0 μM of SAHA was added after 24 h and the cells were then cultured for 72 h. Cells were collected after treating with trypsin (Sigma-Aldrich) and number of cells number was counted using a hemocytometer and the Scepter 2.0 Handheld Cell Counter (Millipore).

CELL VIABILITY ASSAY

The viability of OR6 cells treated with SAHA was analyzed using Vi-CELL XR cell viability counter (Beckman Coulter). Five hundred microliters of cell suspension were mixed with trypan blue, and then images were taken to determine cell concentration and viability.

LUCIFERASE ASSAY

OR6 cells were seeded at 4.0×10^4 cells/well in a 24-well plate for 24 h. SAHA (0.1, 0.5, 0.8, or 1.0 μM) was added and the cells were then cultured for 72 h. Luciferase activity was measured with Renilla Luciferase Assay System (Promega) using a luminometer (Lumat CB 9507, Berthold Technologies). One hundred microliters of Renilla Luciferase Assay Reagent and 20 μl of cell lysate were mixed in tube, and then luminescence was measured. Luciferase activity was normalized with cell number.

RNA EXTRACTION

Total RNA including small RNA was extracted from OR6 cells using the mirVana miRNA isolation kit (Ambion). The sample is first lysed in a denaturing lysis solution which stabilizes RNA and inactivates RNases. The lysate is then extracted once with Acid-Phenol: Chloroform which removes most of the other cellular components, leaving a semi-pure RNA sample. This is further purified over a glass-fiber filter to yield total RNA enriched in miRNAs.

QUANTITATIVE RT-PCR OF *miR-122*

Levels of miRNA expression were analyzed by quantitative RT-PCR using the TaqMan microRNA assay for *miR-122* (Applied Biosystems) according to the manufacturer's instructions. Expression levels were normalized to that of U6 RNA.

MICROARRAY ANALYSIS

Microarray analysis was carried out using the Human Oligo chip 25K (ID QH0ZG35) by Toray (http://www.3d-gene.com/). In brief, total RNA was amplified using an Amino Allyl aRNA kit (Ambion). RNA from SAHA treated cells was labeled with Cy3 Mono-Reactive Dye (GE Healthcare), and control RNA was labeled with Cy5 Mono-Reactive Dye (GE Healthcare). After purification, each 1 μg sample was mixed and hybridized at 37°C for 16 h. After washing, the hybridized chip was scanned using a 3D-Gene Scanner 3000 (Toray). Background was subtracted from the raw data and the values were normalized according to a median Cy3/Cy5 ratio of 1.

QUANTITATIVE RT-PCR OF *OPN* AND *Apo-A1*

After incubation with DNase I (Promega) to eliminate DNA contamination, 1 mg of total RNA was applied for RT reaction with random primers using High Capacity cDNA Reverse Transcription kit (Applied Biosystems). Then, quantitative RT-PCR was performed with

SYBR Green PCR Master Mix (Applied Biosystems) using CFX96 real-time PCR system (Bio-Rad). The primer sequences for quantitative RT-PCR of *OPN* and *Apo-A1* were obtained from the previous reports [Hahnel et al., 2010; Haas et al., 2011]. *GAPDH* was used as an internal control.

OPN forward: 5′-TGGCCGAGGTGATAGTGTG-3′, *OPN* reverse: 5′-CGGGGATGGCCTTGTATG-3′, *Apo-A1* forward: 5′-AGCTTGCTGAAGGTGGAGGT-3′, *Apo-A1* reverse: 5′-ATCGAGTGAAGGACCTGGC-3′, *GAPDH* forward: 5′-CTCCTCCTGTTCGACAGTCAGC-3′, *GAPDH* reverse: 5′-CCCAATACGACCAAATCCGTTG-3′.

The PCR conditions were as follows; *OPN*: 95°C for 15 min, 40-cycles following reaction; 95°C for 30 s, 60°C for 30 s, and 72°C for 30 s. *Apo-A1*: 95°C 3 min, 40 cycles; 95°C for 1 min, 52°C for 1 min, and 72°C for 1 min.

WESTERN BLOTTING OF OPN AND Apo-A1

Protein extracts were separated by SDS/polyacrylamide gel electrophoresis and transferred onto nitrocellulose membranes. Membranes were hybridized with the mouse anti-OPN monoclonal antibody (sc-21742, Santa Cruz Biotechnology) and the goat anti-Apo-A1 polyclonal antibody (ab7613, Abcam). β-actin was used as the internal control.

CHROMATIN IMMUNOPRECIPITATION (ChIP) ASSAY

ChIP assay for acetylation of histone H3 around the promoter region of *OPN* was performed using acetyl-histone H3 ChIP assay kit (Millipore) according to the manufacturer's instructions. In brief, 1×10^7 of OR6 cells were cross-linked with 1% formaldehyde at 37°C for 10 min. Crude cell lysates were sonicated to generate DNA fragments of 200–1,000 bp. ChIP was performed with anti-acetyl-histone H3 antibody as well as control IgG. Quantitative PCR analysis was performed with SYBR Green PCR Master Mix (Applied Biosystems) using a CFX96 real-time PCR system (Bio-Rad). The primer sequence for ChIP assay of *OPN* was designed using the UCSC Genome Browser (http://genome.ucsc.edu/) and the Primer3 (http://frodo.wi.mit.edu/).

OPN (ChIP) forward: 5′-TCATACAGGCAAGAGTGGTTGCAGA-3′, *OPN* (ChIP) reverse: 5′-GCTCCCACACTTCCCCCTCTGGTTT-3′.

The primer sequence for ChIP assay of *Apo-A1* was obtained from the previous report [Mishiro et al., 2009].

Apo-A1 (ChIP) forward: 5′-CAAGGCCTGAACCTTGAGC-3′, *Apo-A1* (ChIP) reverse: 5′-TTAGAGACTGCGAGAAGGAGGT-3′.

The PCR conditions were as follows; 95°C for 3 min, 40-cycles following reaction; 95°C for 30 s, 60°C for 30 s, and 72°C for 30 s. The fraction of immunoprecipitated DNA was calculated as follows: [immunoprecipitated DNA (IP) with anti-acetyl-histone H3 antibody–nonspecific antibody control (NAC)]/(input DNA–NAC). Fold changes relative to control that was set to 1.0 were compared.

TRANSFECTION OF THE *OPN* EXPRESSION VECTOR AND THE *Apo-A1* siRNA

The expression vector containing the *OPN* open reading flame and the pre-designed siRNA for the *Apo-A1* gene (#s1467) were purchased from InvivoGen and Ambion, respectively. They were transfected into OR6 cells using lipofectamine (Invitrogen) in accordance with the manufacturer's instructions. Forty-eight hours after transfection, the cells were collected and luciferase activity was analyzed as described above. OR6 cells treated with lipofectamine only were used as controls.

STATISTICS

The data were expressed as mean and standard deviation (SD) for at least three independent experiments. The data were analyzed using the SPSS statistics software and differences with P values of less than 0.05 were considered significant.

RESULTS

TREATMENT OF OR6 CELLS WITH 1.0 MM OF SAHA DID NOT AFFECT CELL VIABILITY

To investigate the cellular toxicity of SAHA in OR6 cells, MTT assay was performed, and the results showed no significant difference in absorbance at concentrations less than 1.5 μM of SAHA, whereas the absorbance at 3 and 5 μM was significantly reduced ($P < 0.01$, Fig. 1A).

We next examined cell number and cell viability after treatment with SAHA using Scepter Handheld Cell Counter and Vi-CELL autoanalyzer, respectively. Cell viability did not differ after treatment with 1.0 μM of SAHA for 72 h as compared to control (Fig. 1B). We also confirmed that there was no significant difference in cell number among control cells and cells treated with 1.0 μM of SAHA and 0.1 μM of another HDAC inhibitor TSA for 24, 48, and 72 h (Fig. 1C). These findings indicate that treatment with SAHA at concentration of 1.0 μM for 72 h did not affect the viability of OR6 cells.

TREATMENT OF OR6 CELLS WITH SAHA AND TSA REDUCED HCV REPLICATION

We next evaluated HCV replication by measuring luciferase activity in OR6 cells. Luciferase activity of OR6 cells was measured after treatment with SAHA at concentrations of 0.1, 0.5, 0.8, or 1.0 μM for 72 h. As shown in Figure 2A, treatment of OR6 cells with SAHA (<1.0 μM) reduced luciferase activity in a dose-dependent manner. Treatment with SAHA at concentrations of 1.0 and 0.8 μM significantly reduced luciferase activity compared to control (Fig. 2A, 1.0 μM: $P < 0.01$, 0.8 μM: $P < 0.05$).

To investigate whether the effect of SAHA was agent-specific or a general consequence of HDAC inhibitors, we treated OR6 cells with another HDAC inhibitor TSA at concentrations of 0.1 and 0.5 μM and confirmed that TSA also suppresses HCV replication (Fig. 2B).

LACK OF INVOLVEMENT OF *miR-122* IN THE SUPPRESSIVE EFFECT OF SAHA ON HCV REPLICATION

The liver-specific miRNA *miR-122* has been reported to bind to the 5′ noncoding region of the HCV genome to facilitate replication of the viral RNA [Jopling et al., 2005]. To determine whether the suppressive effect of HDAC inhibitors on HCV replication is mediated through alterations in *miR-122* expression, we performed quantitative RT-PCR to measure *miR-122* expression in OR6 cells cultured with 1 μM SAHA or 0.1 μM TSA for 72 h. As shown in Figure 3, *miR-122* expression did not differ between control cells and cells treated with

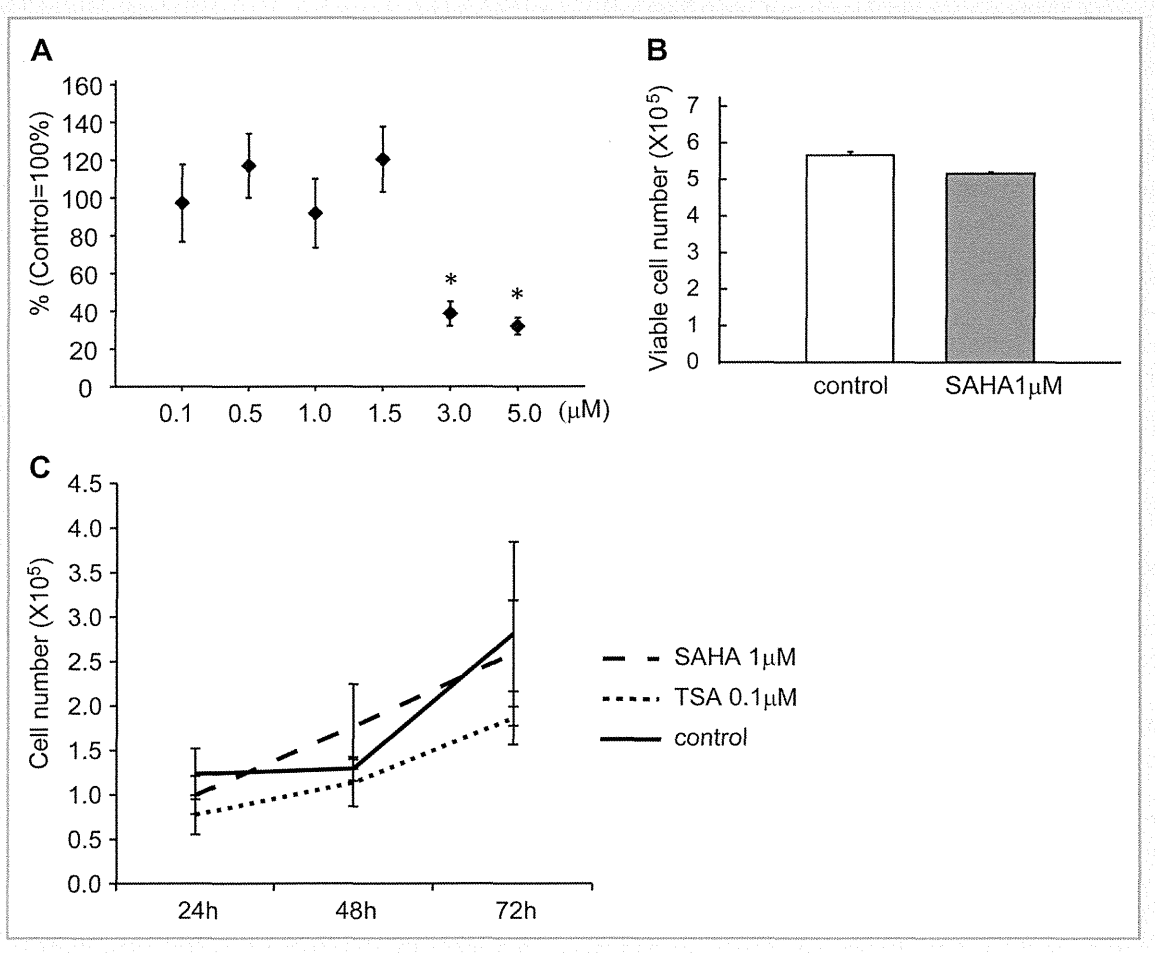

Fig. 1. A: MTT assay for cell viability of OR6 cells after SAHA treatment The viability of OR6 cells was measured by MTT assay. OR6 cells were treated with SAHA at concentrations of 0.1, 0.5, 1.0, 1.5, 3.0, or 5.0 μM for 72 h and MTT assay was then performed to determine the number of viable cells. Absorbance of cells treated with 3.0 and 5.0 μM of SAHA was significantly decreased compared with control. No toxic effect was observed at SAHA concentrations at or below 1 μM. Dots and bar indicate means and SDs for four experiments. $^*P < 0.01$. B: Cell viability of OR6 cells after SAHA treatment OR6 cells were treated with 1 μM SAHA for 72 h. Cell viability was tested using a Vi-CELL autoanalyzer. There was no significant difference in the number of viable cells between the control and 1.0 μM SAHA conditions. Means and SDs of viable cell numbers for three experiments are shown. C: Cell number of OR6 cells treated with 1.0 μM SAHA and 0.1 μM TSA The cell number in OR6 cells treated with 1.0 μM SAHA and 0.1 μM TSA for 24, 48 and 72 h did not differ significantly versus control cells. Cell number was measured by the Scepter Handheld Cell Counter and means and SDs for five experiments are shown.

SAHA or TSA, indicating that *miR-122* is not involved in the suppressive effect of HDAC inhibitors on HCV replication.

ALTERATION OF *OSTEOPONTIN* (*OPN*) AND *APOLIPOPROTEIN-A1* (*Apo-A1*) EXPRESSION LEVELS AFTER TREATMENT OF OR6 CELLS WITH SAHA

To determine comprehensive gene expression changes induced by SAHA treatment, microarray analysis was applied in SAHA-treated OR6 cells (Fig. 4A). We selected genes with expression levels of more than 100 and more than a fourfold difference relative to control. The genes that were up-regulated and down-regulated in SAHA-treated OR6 cells are summarized in Tables I and II. Among genes whose expression was largely changed, we selected genes intimately related to HCV replication from Tables I and II by means of document retrieval. From the literature search, *OPN* was picked-up from the up-regulated genes since *OPN* is an important cytokine for host resistance to viral infection through the initiation of the Th1 immune response [Patarca et al., 1993; Ashkar et al., 2000]. *Apo-A1* was selected from among the down-regulated genes since *Apo-A1* is closely involved in the HCV life cycle [Mancone et al., 2011].

Quantitative RT-PCR shown in Figure 4B and C demonstrated that expression of *OPN* was significantly up-regulated (8.6-fold, $P < 0.001$), and expression of *Apo-A1* was significantly down-regulated (0.39-fold, $P < 0.001$) by treatment with 1 μM SAHA for 72 h. We confirmed the increased protein expression of OPN and the decreased protein expression of Apo-A1 after treatment with 1 μM SAHA by Western blotting (Fig. 4B,C). To investigate whether the changes in expression of these two genes affect HCV RNA replication in OR6 cells, we overexpressed the *OPN* gene using the expression vector containing the *OPN* open reading frame and knocked down the *Apo-A1* gene using the specific siRNA in OR6 cells and examined

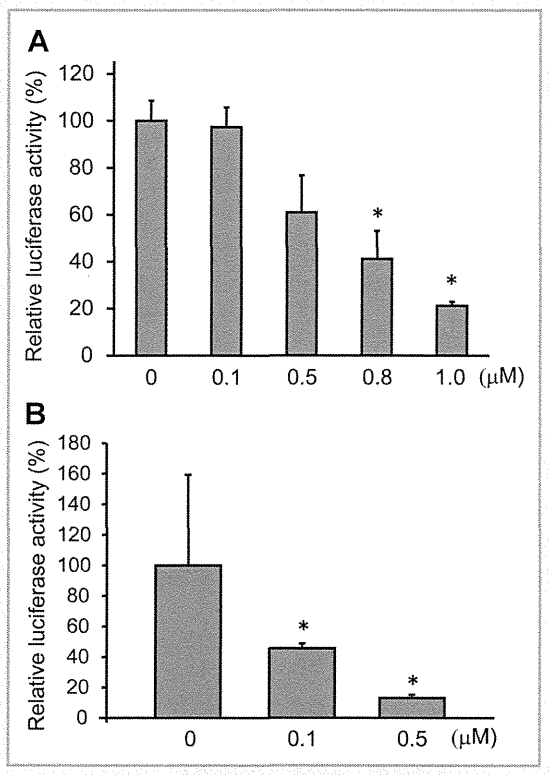

Fig. 2. A: HCV replication in OR6 cells after SAHA treatment HCV replication was evaluated by luciferase activity in OR6 cells treated with SAHA. OR6 cells were treated with 0.1, 0.5, 0.8, or 1.0 μM SAHA for 72 h and luciferase activity was measured. Means and SDs of luciferase activities for three experiments are shown. Luciferase activity in SAHA-treated OR6 cells was dose-dependently reduced, and the reduction at concentrations of 0.8 and 1.0 μM were statistically significant. *$P < 0.05$. B: HCV replication in OR6 cells after TSA treatment HCV replication was evaluated by luciferase activity in OR6 cells treated with TSA. Means and SDs of luciferase activities for three experiments are shown. OR6 cells were treated with 0.1 and 0.5 μM TSA, and the luciferase activity in TSA-treated OR6 cells was significantly reduced. *$P < 0.05$.

changes in luciferase activity. As shown in Figure 5A,B, we confirmed overexpression of OPN and knockdown of Apo-A1 after transfection of *OPN*-expressing vector and siRNA for *Apo-A1*, respectively. After transfection of *OPN*-expressing vector, luciferase activity was significantly reduced to around 40% of control ($P < 0.01$), and knockdown of *Apo-A1* by siRNA resulted in decrease of luciferase activity to around 60% of control ($P < 0.05$).

INCREASED HISTONE H3 ACETYLATION AT THE PROMOTER REGIONS OF *OPN* AND *Apo-A1* AFTER TREATMENT OF OR6 CELLS WITH SAHA

Since histone acetylation generally activates gene expression, we further examined histone acetylation levels around the promoter regions of *OPN* and *Apo-A1* by ChIP assay in OR6 cells treated with 1 μM SAHA.

We designed the ChIP primers according to the report of Liang et al. [2004]. They have demonstrated that histone H3 acetylation is localized within 500 bp of transcriptional start sites (TSSs) of transcriptionally active genes. Therefore we designed the ChIP primers within 500 bp of TSSs of the *OPN* gene and the *Apo-A1* gene, and confirmed the location of the ChIP primers using the UCSC Genome Browser (http://genome.ucsc.edu/). The ChIP-PCR products for the *OPN* gene and the *Apo-A1* gene are 279 and 78 bp, respectively (Fig. 6A,B).

The results of the ChIP assay showed that histone H3 acetylation levels of the promoter regions of *OPN* and *Apo-A1* were significantly higher in SAHA-treated OR6 cells compared to control ($P < 0.01$, Fig. 6A,B). These results suggest that up-regulation of the *OPN* gene is induced by histone H3 acetylation around its promoter region through SAHA treatment of OR6 cells. Although expression level of *Apo-A1* was significantly decreased after SAHA treatment of OR6 cells, histone H3 acetylation level of the promoter region of *Apo-A1* was increased after SAHA treatment.

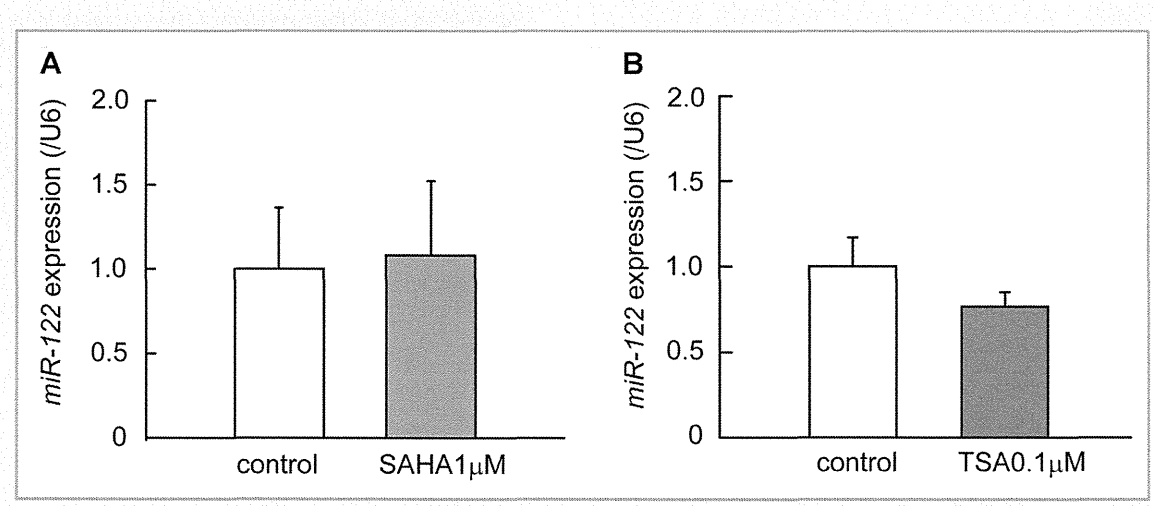

Fig. 3. Expression of *miR-122* in OR6 cells after treatment with SAHA and TSA OR6 cells were treated with 1 μM SAHA (A) or 0.1 μM TSA (B) for 72 h. Expression levels of *miR-122* were examined by TaqMan® quantitative RT-PCR. Means and SDs of *miR-122* expression normalized with U6 for three experiments are shown. There was no significant difference in *miR-122* expression between control and treatment with SAHA or TSA.

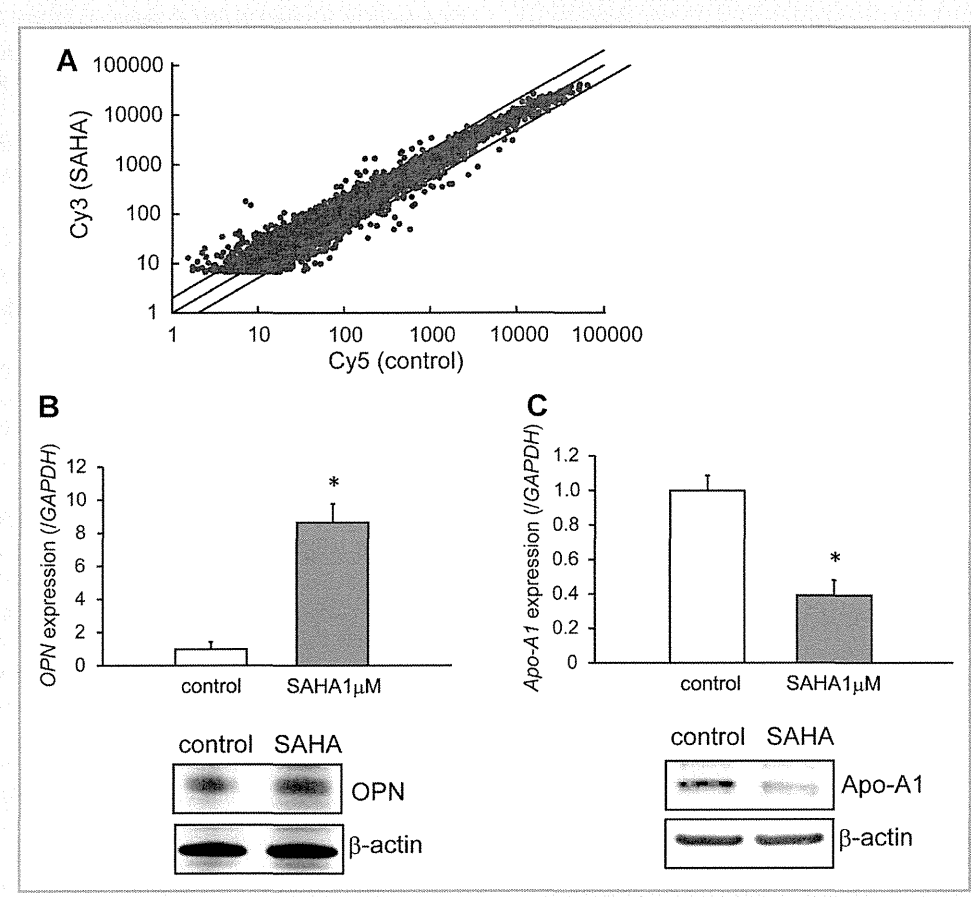

Fig. 4. A: Microarray analysis of OR6 cells after SAHA treatment Standardized data of Cy3 (SAHA)- and Cy5 (control)-stained RNAs are plotted. Global normalization was performed by adjusting to a median Cy3/Cy5 to 1. Lines outside the median line represent twofold difference. Values were normalized according to a median Cy3/Cy5 ratio of 1. B,C: Expression levels of *OPN* and *Apo-A1* in OR6 cells after SAHA treatment Expression levels of *OPN* and *Apo-A1* were examined by quantitative RT-PCR and Western blotting. Means and SDs of gene expression normalized with GAPDH for three experiments are shown. *OPN* expression was significantly up-regulated after treatment with 1 μM SAHA for 72 h compared to control (B: $^*P < 0.001$). *Apo-A1* expression was significantly down-regulated after treatment with 1 μM SAHA for 72 h compared to control (C: $^*P < 0.001$).

DISCUSSION

In the present study, we investigated whether the HDAC inhibitor SAHA affects HCV replication via epigenetic alterations in host cells. To this objective, we used OR6 cells, in which full-length HCV RNA replicates, were used as the replicon system.

The replicon cell culture system was first established by Lohmann et al. [1999] and this system finally developed to the infectious HCV particle producing cell system [Wakita et al., 2005]. In the replicon system, modified HCV genomes can replicate to high levels in human hepatocellular carcinoma cells (HuH-7) and many stably transfected replicon cell lines are established after continuous drug selection with

TABLE I. Up-Regulated Genes in SAHA-Treated OR6 Cells

Name	Description	SAHA/control	$\log_2$ (SAHA/control)	Up
ANXA1	Annexin A1	25.23	4.66	[a]
SPP1	Osteopontin	7.43	2.89	[b]
UBE2L6	Ubiquitin/ISG15-conjugating enzyme E2L6	5.80	2.54	[b]
IFIT1	Interferon-induced rotein with tetratricopeptide repeats 1	5.30	2.40	[b]
TUBA1A	Tubulin alpha-1A chain	4.86	2.28	[b]
KCNJ8	ATP-sensitive inward rectifier potassium channel 8	4.55	2.19	[b]
EFEMP1	EGF-containing fibulin-like extracellular matrix protein 1	4.43	2.12	[b]
KRT23	Keratin, type I cytoskeletal 23	4.07	2.03	[b]

OR6 cells were treated with 1 μM SAHA for 72 h and total RNA was analyzed by microarray (Human Oligo chip 25K). Genes with expression levels of more than 100 and more than a fourfold difference relative to control were selected.
[a]>eightfold.
[b]>fourfold.

TABLE II. Down-Regulated Genes in SAHA-Treated OR6 Cells

Name	Description	SAHA/control	$\log_2$ (SAHA/control)	Down
SERPINC1	Antithrombin-III	0.08	3.58	[a]
GJB1	Gap junction beta-1 protein	0.14	2.80	[b]
F12	Coagulation factor XII	0.17	2.54	[b]
SLCO183	Solute carrier organic anion transporter family member 183	0.22	2.19	[b]
C3	Complement C3	0.22	2.18	[b]
AKR1810	Aldo-keto reductase family 1 member 810	0.23	2.11	[b]
GAL	Galanin	0.24	2.07	[b]
FABP1	Fatty acid-binding protein, liver	0.24	2.06	[b]
APOA1	Apolipoprotein A1	0.25	2.00	[b]

OR6 cells were treated with 1 μM SAHA for 72 h and total RNA was analyzed by microarray (Human Oligo chip 25K). Genes with expression levels of more than 100 and less than 1/4 of control were selected.

[a]<1/16.

[b]<1/4.

neomycin (G418). This cell culture system has been widely used as a tool in the study of HCV virology and drug development [Horscroft et al., 2005]. Development of OR6 cell was originally reported by Ikeda et al. [2005]. The *Renilla* luciferase reporter gene and neomycin resistant gene were introduced in the 5′ untranslated region of genome-length HCV RNA (genotype 1b). This construct containing full-length HCV RNA robustly replicated in the HuH-7 cells after the electroporation and one of the colonies designated OR6 was selected by G418.

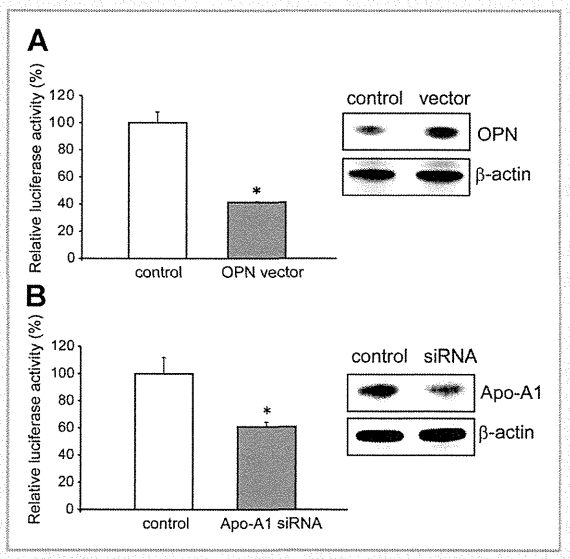

Fig. 5. Reduced HCV replication in OR6 cells after gene transfer. A: HCV replication in OR6 cells after overexpression of the *OPN* gene HCV replication was evaluated by luciferase activity in OR6 cells after transfection with the *OPN* expression vector. Means and SDs of luciferase activities for three experiments are shown. The luciferase activity in OR6 cells after overexpression of the *OPN* gene was significantly reduced. *$P < 0.01$. B: HCV replication in OR6 cells after knockdown of the *Apo-A1* gene HCV replication was evaluated by luciferase activity in OR6 cells after transfection with siRNA for the *Apo-A1* gene. Means and SDs of luciferase activities for three experiments are shown. The luciferase activity in OR6 cells after knockdown of the *Apo-A1* gene was significantly reduced. *$P < 0.05$.

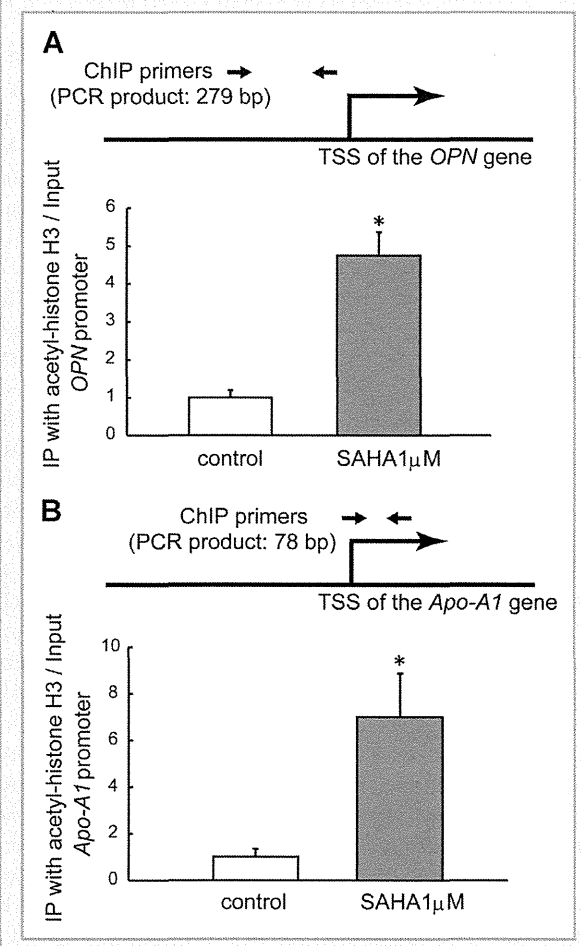

Fig. 6. ChIP assay at the promoter regions of *OPN* and *Apo-A1* in OR6 cells after SAHA treatment levels of acetylated histone H3 around the promoter regions of *OPN* (A) and *Apo-A1* (B) after SAHA treatment were analyzed by ChIP assay. The ChIP primers are located near the TSSs of these genes and should be suitable for histone acetylation assay. The ChIP-PCR products for the *OPN* gene and the *Apo-A1* gene are 279 and 78 bp, respectively. The fraction of immunoprecipitated DNA was calculated as: immunoprecipitated DNA (IP) with anti-acetyl-histone H3 antibody/input DNA. Means and SDs of acetylated histone H3 levels for three experiments are shown. The acetylated histone H3 levels around the promoter regions of *OPN* and *Apo-A1* were significantly increased after SAHA treatment. *$P < 0.001$.

The OR6 cell system facilitates monitoring of HCV RNA replication. However, if cell viability is decreased as a result of drug toxicity, luciferase activity cannot be evaluated accurately. Therefore, we first examined the cellular toxicity of SAHA in OR6 cells and confirmed that SAHA treatment was non-toxic at concentrations below 1 μM as determined by cell counting, viability assay, and MTT assay. Lu et al. have reported the inhibitory effect of HDAC inhibitors including SAHA on hepatocellular carcinoma (HCC). They treated several HCC cell lines with SAHA at various concentrations and show similar results to our results [Lu et al., 2007]. In contrast, the HCV replication rate evaluated by luciferase activity was significantly reduced by treatment with SAHA at concentration below 1 μM in a dose-dependent manner. We also confirmed that another HDAC inhibitor TSA suppresses HCV replication (Fig. 2B). These results indicate that the HDAC inhibitors SAHA and TSA reduced HCV replication without cellular toxicity in OR6 cells.

We next investigated the molecular mechanisms underlying the suppressive effect of SAHA on the HCV replication rate. *miR-122* is a liver-specific miRNA and plays an important role in fatty-acid metabolism in the liver [Esau et al., 2006]. Recent studies have reported that *miR-122* is down-regulated in HCC and has multiple functions as a tumor suppressor during hepatocarcinogenesis [Coulouarn et al., 2009; Fornari et al., 2009]. Moreover, *miR-122* directly binds to the 5′ noncoding region of the HCV genome and modulates HCV RNA replication [Jopling et al., 2005]. It is noteworthy that *miR-122* facilitates HCV replication via binding to the 5′ noncoding region of the viral genome, whereas miRNAs generally function to repress expression of their target genes by binding to 3′ noncoding regions. Epigenetic alterations such as DNA methylation and histone modification are important mechanisms for the regulation of miRNA expression [Saito et al., 2006, 2011]. In this study, we investigated the effect of treatment with HDAC inhibitors on *miR-122* expression in OR6 cells and found that there was no significant difference in *miR-122* expression after treatment with 1 μM SAHA or 0.1 μM TSA, suggesting that *miR-122* is not involved in the suppressive effect of HDAC inhibitors on HCV replication. These findings led us to hypothesize that histone acetylation induced by SAHA treatment does not modulate *miR-122* expression and that HCV replication was inhibited through other pathways.

Microarray analysis showed differential expression of various genes in OR6 cells induced by SAHA treatment for 72 h. Notably, several cytoskeletal genes such as *tubulin alpha-1A chain*, *extracellular matrix protein 1*, and *keratin* were significantly up-regulated by SAHA treatment. We have reported that a close correlation might exist between malignant transformation of HCC and cytoskeletal changes [Kanamori et al., 2011]. The results of this study are similar to those of our previous studies showing that sodium butyrate, another HDAC inhibitor, changed the mobility, fluidity, and adhesive properties of cancer cells into less a malignant phenotype [Saito et al., 1998; Masuda et al., 2000; Wakabayashi et al., 2000; Nakamura et al., 2001; Kaneko et al., 2004]. Another interesting result of the microarray was the up-regulation of interferon-induced protein by SAHA treatment. This finding is also consistent with our previous study, in which sodium butyrate induced interferon-related gene expression [Wakabayashi et al., 2005], suggesting that there may be crosstalk between the interferon-inducing pathway and epigenetic changes by HDAC inhibitors. Up-regulation of interferon-induced protein by HDAC inhibitors may result in suppression of HCV replication.

Besides cytoskeletal genes and interferon-induced proteins, we focused our present study on *OPN* and *Apo-A1*. The *OPN* gene is a key regulator of the Th1-type immune system and Th1-type immunity plays an important role in viral elimination [Patarca et al., 1993; Ashkar et al., 2000]. Recent studies showed that the promoter activity of *OPN* was correlated with the efficacy of interferon-based therapy [Mochida et al., 2004; Naito et al., 2005]. These findings suggest that increased expression of *OPN* can eliminate HCV by activating the Th1-type immune system. Among the genes that were down-regulated by SAHA treatment, we focused on the *Apo-A1* gene because this protein is essential for HCV replication [Mancone et al., 2011]. The *Apo-A1* gene is a protein component of high-density lipoprotein particles and is thought to be necessary for HCV particle formation and maintenance of infectivity. To confirm the results of the microarray analysis, we examined expression of *OPN* and *Apo-A1* in OR6 cells after SAHA treatment by quantitative RT-PCR. We found a significant increase of *OPN* expression and significant reduction of *Apo-A1* expression, which may lead to suppression of HCV replication. Moreover, we overexpressed *OPN* and knocked down *Apo-A1* in OR6 cells using an expression vector and siRNA procedure, respectively. As shown in Figure 5A,B, the luciferase activities were significantly reduced after overexpression of *OPN* and knockdown of *Apo-A1* in OR6 cells. These results indicate that overexpression of *OPN* and reduced expression of *Apo-A1* play critical roles in SAHA-induced suppression of HCV replication.

Since histone acetylation generally activates gene expression, we presumed that up-regulation of *OPN* is mediated by histone H3 acetylation around its promoter region. The ChIP assay results demonstrated that histone H3 acetylation levels of the promoter regions of *OPN* and *Apo-A1* were remarkably increased in SAHA-treated OR6 cells compared to control. Acetylation of lysine residues on histones H3 is correlated with active or open chromatin, which allows various transcription factors access to the promoters of target genes [Yoo and Jones, 2006]. This suggests that up-regulation of *OPN* is induced by histone H3 acetylation through SAHA-mediated epigenetic mechanisms. On the other hand, *Apo-A1* transcription was significantly down-regulated by SAHA treatment in OR6 cells despite acetylation of its promoter region. Although up-regulation of *OPN* expression by SAHA treatment is reasonable, we could not prove the molecular mechanism underlying down-regulation of *Apo-A1* by SAHA treatment at this time. Studies have demonstrated that HDAC inhibitors suppress expression of specific genes such as *adiponectin* and *bcl-2* [Duan et al., 2005; Qiao et al., 2006]. Further studies regarding *Apo-A1* inactivation induced by HDAC inhibitors are necessary.

To our knowledge, this study is the first report showing that the HDAC inhibitor SAHA significantly inhibits HCV replication. We presume that this inhibitory effect on HCV replication may be mediated by up-regulation of *OPN* via SAHA-mediated histone modification in host cells, which is expected to inhibit HCV replication. Another significant benefit of SAHA treatment on HCV replication may be down-regulation of *Apo-A1*, which is essential for the HCV life cycle. These findings suggest that epigenetic therapy

with HDAC inhibitors represents a novel potential treatment strategy for diseases associated with HCV infection such as chronic hepatitis, liver cirrhosis, and HCC.

ACKNOWLEDGMENTS

This work was supported by a Grant-in-Aid for Young Scientists A (23680090 to Y.S.) and Grant-in-Aid for Scientific Research C (#24590993 to H.S.) from the Japan Society for the Promotion of Science (JSPS), the Keio Gijuku Academic Development Fund (to Y.S.), Takeda Science Foundation (to Y.S.), and Inaida Foundation (H.S.).

REFERENCES

Ashkar S, Weber GF, Panoutsakopoulou V, Sanchirico ME, Jansson M, Zawaideh S, Rittling SR, Denhardt DT, Glimcher MJ, Cantor H. 2000. Eta-1 (osteopontin): An early component of type-1 (cell-mediated) immunity. Science 287:860–864.

Butler LM, Zhou X, Xu WS, Scher HI, Rifkind RA, Marks PA, Richon VM. 2002. The histone deacetylase inhibitor SAHA arrests cancer cell growth, up-regulates thioredoxin-binding protein-2, and down-regulates thioredoxin. Proc Natl Acad Sci USA 99:11700–11705.

Chen YC, Su WC, Huang JY, Chao TC, Jeng KS, Machida K, Lai MM. 2010. Polo-like kinase 1 is involved in hepatitis C virus replication by hyper-phosphorylating NS5A. J Virol 84:7983–7993.

Coulouarn C, Factor VM, Andersen JB, Durkin ME, Thorgeirsson SS. 2009. Loss of miR-122 expression in liver cancer correlates with suppression of the hepatic phenotype and gain of metastatic properties. Oncogene 28:3526–3536.

Duan H, Heckman CA, Boxer LM. 2005. Histone deacetylase inhibitors down-regulate bcl-2 expression and induce apoptosis in t(14;18) lymphomas. Mol Cell Biol 25:1608–1619.

Ebinuma H, Saito H, Tada S, Nakamoto N, Ohishi T, Tsunematsu S, Kumagai N, Tsuchimoto K, Tsukada N, Inagaki Y, Horie Y, Takahashi M, Atsukawa K, Okamura Y, Kanai T, Hibi T. 2012. Disadvantages of peginterferon and ribavirin treatment in older patients with chronic hepatitis C: An analysis using the propensity score. Hepatol Int 6:744–752.

Esau C, Davis S, Murray SF, Yu XX, Pandey SK, Pear M, Watts L, Booten SL, Graham M, McKay R, Subramaniam A, Propp S, Lollo BA, Freier S, Bennett CF, Bhanot S, Monia BP. 2006. miR-122 regulation of lipid metabolism revealed by in vivo antisense targeting. Cell Metab 3:87–98.

Fornari F, Gramantieri L, Giovannini C, Veronese A, Ferracin M, Sabbioni S, Calin GA, Grazi GL, Croce CM, Tavolari S, Chieco P, Negrini M, Bolondi L. 2009. MiR-122/cyclin G1 interaction modulates p53 activity and affects doxorubicin sensitivity of human hepatocarcinoma cells. Cancer Res 69:5761–5767.

Gal-Yam EN, Saito Y, Egger G, Jones PA. 2008. Cancer epigenetics: Modifications, screening, and therapy. Annu Rev Med 59:267–280.

Gao L, Aizaki H, He JW, Lai MM. 2004. Interactions between viral nonstructural proteins and host protein hVAP-33 mediate the formation of hepatitis C virus RNA replication complex on lipid raft. J Virol 78:3480–3488.

Haas MJ, Alamir AR, Sultan S, Chehade JM, Wong NC, Mooradian AD. 2011. Nicotinic acid induces apolipoprotein A-I gene expression in HepG2 and Caco-2 cell lines. Metabolism 60:1790–1796.

Hahnel A, Wichmann H, Kappler M, Kotzsch M, Vordermark D, Taubert H, Bache M. 2010. Effects of osteopontin inhibition on radiosensitivity of MDA-MB-231 breast cancer cells. Radiat Oncol 5:82.

Hamamoto I, Nishimura Y, Okamoto T, Aizaki H, Liu M, Mori Y, Abe T, Suzuki T, Lai MM, Miyamura T, Moriishi K, Matsuura Y. 2005. Human VAP-B is involved in hepatitis C virus replication through interaction with NS5A and NS5B. J Virol 79:13473–13482.

Horscroft N, Lai VC, Cheney W, Yao N, Wu JZ, Hong Z, Zhong W. 2005. Replicon cell culture system as a valuable tool in antiviral drug discovery against hepatitis C virus. Antivir Chem Chemother 16:1–12.

Ikeda M, Abe K, Dansako H, Nakamura T, Naka K, Kato N. 2005. Efficient replication of a full-length hepatitis C virus genome, strain O, in cell culture, and development of a luciferase reporter system. Biochem Biophys Res Commun 329:1350–1359.

Ikeda M, Abe K, Yamada M, Dansako H, Naka K, Kato N. 2006. Different anti-HCV profiles of statins and their potential for combination therapy with interferon. Hepatology 44:117–125.

Jopling CL, Yi M, Lancaster AM, Lemon SM, Sarnow P. 2005. Modulation of hepatitis C virus RNA abundance by a liver-specific MicroRNA. Science 309:1577–1581.

Kanamori H, Kawakami T, Effendi K, Yamazaki K, Mori T, Ebinuma H, Masugi Y, Du W, Nagasaka K, Ogiwara A, Kyono Y, Tanabe M, Saito H, Hibi T, Sakamoto M. 2011. Identification by differential tissue proteome analysis of talin-1 as a novel molecular marker of progression of hepatocellular carcinoma. Oncology 80:406–415.

Kaneko F, Saito H, Saito Y, Wakabayashi K, Nakamoto N, Tada S, Suzuki H, Tsunematsu S, Kumagai N, Ishii H. 2004. Down-regulation of matrix-invasive potential of human liver cancer cells by type I interferon and a histone deacetylase inhibitor sodium butyrate. Int J Oncol 24:837–845.

Kaul A, Stauffer S, Berger C, Pertel T, Schmitt J, Kallis S, Zayas M, Lohmann V, Luban J, Bartenschlager R. 2009. Essential role of cyclophilin A for hepatitis C virus replication and virus production and possible link to polyprotein cleavage kinetics. PLoS Pathog 5:e1000546.

Kurita S, Higuchi H, Saito Y, Nakamoto N, Takaishi H, Tada S, Saito H, Gores GJ, Hibi T. 2010. DNMT1 and DNMT3b silencing sensitizes human hepatoma cells to TRAIL-mediated apoptosis via up-regulation of TRAIL-R2/DR5 and caspase-8. Cancer Sci 101:1431–1439.

Lauer GM, Walker BD. 2001. Hepatitis C virus infection. N Engl J Med 345: 41–52.

Liang G, Lin JC, Wei V, Yoo C, Cheng JC, Nguyen CT, Weisenberger DJ, Egger G, Takai D, Gonzales FA, Jones PA. 2004. Distinct localization of histone H3 acetylation and H3-K4 methylation to the transcription start sites in the human genome. Proc Natl Acad Sci USA 101:7357–7362.

Lohmann V, Korner F, Koch J, Herian U, Theilmann L, Bartenschlager R. 1999. Replication of subgenomic hepatitis C virus RNAs in a hepatoma cell line. Science 285:110–113.

Lu YS, Kashida Y, Kulp SK, Wang YC, Wang D, Hung JH, Tang M, Lin ZZ, Chen TJ, Cheng AL, Chen CS. 2007. Efficacy of a novel histone deacetylase inhibitor in murine models of hepatocellular carcinoma. Hepatology 46:1119–1130.

Mancone C, Steindler C, Santangelo L, Simonte G, Vlassi C, Longo MA, D'Offizi G, Di Giacomo C, Pucillo LP, Amicone L, Tripodi M, Alonzi T. 2011. Hepatitis C virus production requires apolipoprotein A-I and affects its association with nascent low-density lipoproteins. Gut 60:378–386.

Masuda T, Saito H, Kaneko F, Atsukawa K, Morita M, Inagaki H, Kumagai N, Tsuchimoto K, Ishii AH. 2000. Up-regulation of E-cadherin and I-catenin in human hepatocellular carcinoma cell lines by sodium butyrate and interferon-alpha. In Vitro Cell Dev Biol Anim 36:387–394.

Mishiro T, Ishihara K, Hino S, Tsutsumi S, Aburatani H, Shirahige K, Kinoshita Y, Nakao M. 2009. Architectural roles of multiple chromatin insulators at the human apolipoprotein gene cluster. EMBO J 28:1234–1245.

Mochida S, Hashimoto M, Matsui A, Naito M, Inao M, Nagoshi S, Nagano M, Egashira T, Mishiro S, Fujiwara K. 2004. Genetic polymorphims in promoter region of osteopontin gene may be a marker reflecting hepatitis activity in chronic hepatitis C patients. Biochem Biophys Res Commun 313:1079–1085.

Naito M, Matsui A, Inao M, Nagoshi S, Nagano M, Ito N, Egashira T, Hashimoto M, Mishiro S, Mochida S, Fujiwara K. 2005. SNPs in the promoter region of the osteopontin gene as a marker predicting the efficacy of interferon-based therapies in patients with chronic hepatitis C. J Gastroenterol 40:381–388.

Nakamura M, Saito H, Ebinuma H, Wakabayashi K, Saito Y, Takagi T, Nakamoto N, Ishii H. 2001. Reduction of telomerase activity in human liver cancer cells by a histone deacetylase inhibitor. J Cell Physiol 187:392–401.

Nakamura M, Saito H, Ikeda M, Tada S, Kumagai N, Kato N, Shimotohno K, Hibi T. 2008. Possible molecular mechanism of the relationship between NS5B polymorphisms and early clearance of hepatitis C virus during interferon plus ribavirin treatment. J Med Virol 80:632–639.

Okamoto T, Nishimura Y, Ichimura T, Suzuki K, Miyamura T, Suzuki T, Moriishi K, Matsuura Y. 2006. Hepatitis C virus RNA replication is regulated by FKBP8 and Hsp90. EMBO J 25:5015–5025.

Patarca R, Saavedra RA, Cantor H. 1993. Molecular and cellular basis of genetic resistance to bacterial infection: the role of the early T-lymphocyte activation-1/osteopontin gene. Crit Rev Immunol 13:225–246.

Qiao L, Schaack J, Shao J. 2006. Suppression of adiponectin gene expression by histone deacetylase inhibitor valproic acid. Endocrinology 147:865–874.

Saito H, Ebinuma H, Takahashi M, Kaneko F, Wakabayashi K, Nakamura M, Ishii H. 1998. Loss of butyrate-induced apoptosis in human hepatoma cell lines HCC-M and HCC-T having substantial Bcl-2 expression. Hepatology 27:1233–1240.

Saito Y, Liang G, Egger G, Friedman JM, Chuang JC, Coetzee GA, Jones PA. 2006. Specific activation of microRNA-127 with downregulation of the proto-oncogene BCL6 by chromatin-modifying drugs in human cancer cells. Cancer Cell 9:435–443.

Saito Y, Suzuki H, Matsuura M, Sato A, Kasai Y, Yamada K, Saito H, Hibi T. 2011. MicroRNAs in hepatobiliary and pancreatic cancers. Front Genet 2:66.

Sarasin-Filipowicz M, Krol J, Markiewicz I, Heim MH, Filipowicz W. 2009. Decreased levels of microRNA miR-122 in individuals with hepatitis C responding poorly to interferon therapy. Nat Med 15:31–33.

Schickel R, Boyerinas B, Park SM, Peter ME. 2008. MicroRNAs: Key players in the immune system, differentiation, tumorigenesis and cell death. Oncogene 27:5959–5974.

Takayama T, Ebinuma H, Tada S, Yamagishi Y, Wakabayashi K, Ojiro K, Kanai T, Saito H, Hibi T. 2011. Prediction of effect of pegylated interferon alpha-2b plus ribavirin combination therapy in patients with chronic hepatitis C infection. PLoS ONE 6:e27223.

Tu H, Gao L, Shi ST, Taylor DR, Yang T, Mircheff AK, Wen Y, Gorbalenya AE, Hwang SB, Lai MM. 1999. Hepatitis C virus RNA polymerase and NS5A complex with a SNARE-like protein. Virology 263:30–41.

Vaillancourt FH, Brault M, Pilote L, Uyttersprot N, Gaillard ET, Stoltz JH, Knight BL, Pantages L, McFarland M, Breitfelder S, Chiu TT, Mahrouche L, Faucher AM, Cartier M, Cordingley MG, Bethell RC, Jiang H, White PW, Kukolj G. 2012. Evaluation of phosphatidylinositol-4-kinase IIIalpha as a hepatitis C virus drug target. J Virol 86:11595–11607.

Wakabayashi K, Saito H, Ebinuma H, Saito Y, Takagi T, Nakamura M, Umezawa A, Hata J, Ishii H. 2000. Bcl-2 related proteins are dramatically induced at the early stage of differentiation in human liver cancer cells by a histone deacetylase inhibitor projecting an anti-apoptotic role during this period. Oncol Rep 7:285–288.

Wakabayashi K, Saito H, Kaneko F, Nakamoto N, Tada S, Hibi T. 2005. Gene expression associated with the decrease in malignant phenotype of human liver cancer cells following stimulation with a histone deacetylase inhibitor. Int J Oncol 26:233–239.

Wakita T, Pietschmann T, Kato T, Date T, Miyamoto M, Zhao Z, Murthy K, Habermann A, Krausslich HG, Mizokami M, Bartenschlager R, Liang TJ. 2005. Production of infectious hepatitis C virus in tissue culture from a cloned viral genome. Nat Med 11:791–796.

Watanabe T, Kato H, Kobayashi Y, Yamasaki S, Morita-Hoshi Y, Yokoyama H, Morishima Y, Ricker JL, Otsuki T, Miyagi-Maesima A, Matsuno Y, Tobinai K. 2010. Potential efficacy of the oral histone deacetylase inhibitor vorinostat in a phase I trial in follicular and mantle cell lymphoma. Cancer Sci 101:196–200.

Yoo CB, Jones PA. 2006. Epigenetic therapy of cancer: Past, present and future. Nat Rev Drug Discov 5:37–50.

JVI
Journals.ASM.org

Hepatitis C Virus Infection Induces Inflammatory Cytokines and Chemokines Mediated by the Cross Talk between Hepatocytes and Stellate Cells

Hironori Nishitsuji,[a] Kenji Funami,[b] Yuko Shimizu,[a] Saneyuki Ujino,[a] Kazuo Sugiyama,[c] Tsukasa Seya,[b] Hiroshi Takaku,[d] Kunitada Shimotohno[a]

Research Center for Hepatitis and Immunology, National Center for Global Health and Medicine, Ichikawa, Chiba, Japan[a]; Department of Microbiology and Immunology, Hokkaido University Graduate School of Medicine, Kita, Sapporo, Japan[b]; Center for Integrated Medical Research, Keio University, Shinjuku-ku, Tokyo, Japan[c]; Department of Life and Environmental Sciences, Chiba Institute of Technology, Narashino-shi, Chiba, Japan[d]

Inflammatory cytokines and chemokines play important roles in inflammation during viral infection. Hepatitis C virus (HCV) is a hepatotropic RNA virus that is closely associated with chronic liver inflammation, fibrosis, and hepatocellular carcinoma. During the progression of HCV-related diseases, hepatic stellate cells (HSCs) contribute to the inflammatory response triggered by HCV infection. However, the underlying molecular mechanisms that mediate HSC-induced chronic inflammation during HCV infection are not fully understood. By coculturing HSCs with HCV-infected hepatocytes *in vitro*, we found that HSCs stimulated HCV-infected hepatocytes, leading to the expression of proinflammatory cytokines and chemokines such as interleukin-6 (IL-6), IL-8, macrophage inflammatory protein 1α (MIP-1α), and MIP-1β. Moreover, we found that this effect was mediated by IL-1α, which was secreted by HSCs. HCV infection enhanced production of CCAAT/enhancer binding protein (C/EBP) β mRNA, and HSC-dependent IL-1α production contributed to the stimulation of C/EBPβ target cytokines and chemokines in HCV-infected hepatocytes. Consistent with this result, knockdown of mRNA for C/EBPβ in HCV-infected hepatocytes resulted in decreased production of cytokines and chemokines after the addition of HSC conditioned medium. Induction of cytokines and chemokines in hepatocytes by the HSC conditioned medium required a yet to be identified postentry event during productive HCV infection. The cross talk between HSCs and HCV-infected hepatocytes is a key feature of inflammation-mediated, HCV-related diseases.

Hepatitis C virus (HCV) can cause chronic liver disease, which can progress to fibrosis, cirrhosis, and hepatocellular carcinoma (HCC) (1). Clearance of HCV during the acute phase of infection is associated with a robust CD4 and CD8 T-cell response to multiple viral epitopes (2). However, clearance of HCV infection often fails because of an intermediate cytotoxic T-cell response that is unable to eliminate the infection but causes hepatocyte destruction. T-cell-mediated hepatocytotoxicity poses a high risk for progression to chronic liver inflammation and damage (3). During chronic HCV infection, chemokine-chemokine receptor interactions are particularly important for the recruitment of T cells to sites of inflammation in the liver. Liver-infiltrating lymphocytes in HCV patients exhibit increased expression of CXCR3 and CCR5 (4). Moreover, intrahepatic chemokines, such as RANTES, macrophage inflammatory protein 1α (MIP-1α), MIP-1β, and IP-10, are elevated in HCV patients (5), and intrahepatic proinflammatory cytokine levels are correlated with the severity of inflammation and liver fibrosis (6).

The induction of proinflammatory cytokines and chemokines is triggered by viral proteins and double-stranded RNA (dsRNA) from HCV. The HCV core protein induces inflammatory cytokines through the STAT3 signaling pathway (7). Retinoic acid-inducible gene I (RIG-I) and Toll-like receptor 3 (TLR-3) are cellular sensors that recognize HCV dsRNA, resulting in production of chemokines such as interleukin-8 (IL-8), RANTES, MIP-1α, and MIP-1β (8, 9). Recently, an alternative mechanism for HCV-induced inflammation was reported. It was demonstrated that NS5B, the viral RNA-dependent RNA polymerase (RdRp), catalyzes production of small RNA species that trigger an innate immune response, leading to the production of both interferon (IFN) and inflammatory cytokines (10).

Hepatic stellate cells (HSCs) represent 5 to 8% of the total human liver cells and reside in the Disse space (11). Activation or transdifferentiation of HSCs is regulated by growth factors, including transforming growth factor β (TGF-β), which are associated with pathological conditions such as liver injury, cirrhosis, and cancer (11, 12). During liver injury, quiescent HSCs become activated and convert into highly proliferative, myofibroblast-like cells, which produce inflammatory and fibrogenic mediators (13). In a human hepatoma model, the cross talk between tumor hepatocytes and activated HSCs induced an inflammatory response, and the amounts of cytokines and chemokines associated with hepatocyte-HSC cross talk correlated to HCC progression (14).

Although direct induction of liver inflammation by HCV infection through cellular sensors or HCV proteins is well documented, little is known about the mechanisms governing the proinflammatory cytokines and chemokines that are produced during the interactions between HCV-infected hepatocytes and HSCs. Here, we show that HSCs can act as an inflammatory mediator to HCV-infected cells. Infection of hepatocytes with HCV

Received 9 April 2013 Accepted 9 May 2013
Published ahead of print 15 May 2013
Address correspondence to Hironori Nishitsuji, lbnishitsuji@hospk.ncgm.go.jp, or Kunitada Shimotohno, lbshimotohno@hospk.ncgm.go.jp.
Copyright © 2013, American Society for Microbiology. All Rights Reserved.
doi:10.1128/JVI.00974-13

resulted in increased CCAAT/enhancer binding protein (C/EBPβ) production. Conditioned medium (CM) from HSCs induced hepatocyte production of inflammatory cytokines and chemokines, such as IL-6, IL-8, and MIP-1β, which are potential targets of C/EBPβ. Stimulation of these cytokines and chemokines in HCV-infected cells by HSC CM was suppressed by knockdown of mRNA for C/EBPβ. From the chemokines secreted by HSCs, IL-1α was identified as the inducer of MIP-1β. These results suggest HSCs may contribute to virus infection-associated liver inflammation through cross talk with HCV-infected hepatocytes.

MATERIALS AND METHODS

Cells. LX2 cells (kindly provided by S. Friedman), NP-2-CCR5 cells (kindly provided by T. Hoshino), and Huh7.5 cells (kindly provided by C. Rice) were cultured in Dulbecco's modified Eagle's medium (DMEM) (Invitrogen) supplemented with 10% fetal bovine serum (FBS), 100 μg/ml penicillin and streptomycin, and 100 U/ml nonessential amino acids (Invitrogen). To maintain the quality of the cells, stored frozen stocks were thawed every 3 months and used in the experiments.

Plasmids. DNA fragments encoding each of the HCV nonstructural proteins were generated from a full-length cDNA clone of JFH1 by PCR. The fragments were cloned into pCAG-GS/N-Flag, in which the sequence encoding a Flag tag is inserted at the 5′ terminus of the cloning site of pCAG-GS.

Virus. Infectious HCV in cell culture (HCVcc) was produced by transfection of Huh7.5 cells with *in vitro*-transcribed RNA derived from JFH1 (kindly provided by T. Wakita) or TNS2J1 (the chimeric HCV genome containing HCV-1b in the structure region and JFH1 non-structural-protein-coding regions). UV-irradiated JFH1 was prepared by irradiation with a UV lamp of 254-nm wavelength at a distance of 6 cm for 1 min.

HCV infection. Huh7.5 cells were infected with JFH1 at a multiplicity of infection (MOI) of 5. Under this condition, 80 to 90% of the cells became positive for HCV core protein after 3 days.

Preparation of conditioned medium from Huh7.5 or LX2 cells. Huh7.5 or LX2 cells (1×10^6) were seeded in 10 ml of medium in a 100-mm dish for 3 days. Supernatants were collected and filtered through 0.45-μm-pore-size filters.

Chemotaxis of NP-2-CCR5 cells. A 60-fold concentration of Huh7.5 or LX2 CM was generated by tapping in a filter membrane that cut off the 100-kDa-molecular-mass marker protein (100,000-molecular-weight-cutoff filter) and was used for experimental stimulations. Huh7.5 or JFH1-infected Huh7.5 cells (Huh7.5/JFH1 cells) were treated with each concentrated CM. After 24 h of treatment, the medium was changed to serum-free DMEM for 24 h and then used for chemotaxis assays. Chemotaxis of NP-2-CCR5 cells was measured in a 48-well chemotaxis chamber (Neuro Probe). The chamber consisted of a 48-well upper chamber and a 48-well lower chamber separated by a polycarbonate filter (pore size, 8 μm) coated with rat tail collagen. The lower wells were filled with each conditioned medium. The NP-2-CCR5 cells were washed and suspended in serum-free DMEM in the absence or presence of 0.1 nM maraviroc and then divided in the upper wells (5,000 cells per well). After incubation at 37°C for 180 min, the cells that had migrated into the lower well of the 48-well chemotaxis chamber were counted by Diff-Quik staining.

Quantitative RT-PCR. Total RNA was extracted from cells using RNeasy minikits (Qiagen), and cDNA was prepared with SuperscriptIII (Invitrogen) using oligo(dT) primers. Quantitative real-time PCR (qRT-PCR) was performed with Fast SYBR green master mix (Applied Biosystems), and fluorescent signals were analyzed with the Fast RT-PCR system (Applied Biosystems). The PCR primer pairs are described in Table 1.

siRNA transfection. Small interfering RNA (siRNA) was transfected using Lipofectamine RNAiMAX reagent (Invitrogen) according to the manufacturer's protocol. The duplex nucleotides of siRNA specific to the mRNA for C/EBPβ (5′-GAAGAAACGUCUAUGUGUA-3′) and the Mission siRNA universal negative control were purchased from Sigma. Synthetic siRNA specific to mRNA for IL-1 receptor-associated kinase 1 (IRAK1) (5′-CCCGGGCAAUUCAGUUUCUACAUCA-3′) and the Stealth RNA interference (RNAi) negative control duplex were purchased from Invitrogen.

TABLE 1 Real-time PCR primers

Primer	Sequence (5′–3′)
CXCL1-F	GCAGGGAATTCACCCCAAGAAC
CXCL1-R	CTATGGGGGATGCAGGATTGAG
CXCL2-F	CCAACTGACCAGAAGGAAGGAG
CXCL2-R	ATGGCCTCCAGGTCATCATCAG
CXCL5-F	TGAGAGAGCTGCGTTGCGTTTG
CXCL5-R	TTCCTTCCCGTTCTTCAGGGAG
CXCL6-F	CTGCGTTGCACTTGTTTACGCG
CXCL6-R	GGGTCCAGACAAACTTGCTTCC
IL-1alpha-F	AGCTATGGCCCACTCCATGAAG
IL-1alpha-R	ACATTAGGCGCAATCCAGGTGG
IL-6-F	CCCCCAGGAGAAGATTCCAAAG
IL-6-R	TTCTGCCAGTGCCTCTTTGCTG
IL-7-F	ATTCCGTGCTGCTCGCAAGTTG
IL-7-R	AACCTGGCCAGTGCAGTTCAAC
IL-8-F	CTGTTAAATCTGGCAACCCTAGTCT
IL-8-R	CAAGGCACAGTGGAACAAGGA
MIP-1alpha-F	GCTGACTACTTTGAGACGAGC
MIP-1alpha-R	CCAGTCCATAGAAGAGGTAGC
MIP-1beta-F	CAGCGCTCTCAGCACCAATGG
MIP-1beta-R	GATCAGCACAGACTTGCTTGCTTC
C/EBP-beta-F	CTCGCAGGTCAAGAGCAAG
C/EBP-beta-R	GACAGCTGCTCCACCTTCTT
Collagen-F	AACATGACCAAAAACCAAAAGTG
Collagen-R	CATTGTTTCCTGTGTCTTCTGG
IL-1R-F	CCTGTCTTATGGCGTTGCAGGC
IL-1R-R	AGTGCCCTGGGCTGCTATTGAC

Cytokine antibody array. LX2 cells (1×10^6) were seeded in 10 ml of medium in a 100-mm dish for 2 days. The supernatant was then changed to 0.2% FBS-DMEM. Two days after incubation, the supernatants were collected and then concentrated by using a 100,000-molecular-weight-cutoff filter. The trapped and flowthrough fractions were dialyzed with phosphate-buffered saline (PBS) for 18 h. The amount of protein in each fraction was determined using a bicinchoninate protein assay kit (Nacalai Tesque). Three milligrams of each fraction was subjected to the cytokine antibody array.

The expression levels of 507 human proteins in the trap and flowthrough fractions from the LX2 cells were determined using biotin label-based human antibody array I (Raybiotech) according to the manufacturer's protocol.

RESULTS

LX2 cells induce MIP-1β expression in JFH1-infected Huh7.5 cells. Our preliminary results indicated that coculturing human hepatic stellate cells (HSCs) with HCV-infected cells stimulated the expression of MIP-1β, which was found to be one of most upregulated chemokines. Here, we focused on its role as a marker of inflammation.

To investigate whether human HSCs play a role in the proinflammatory response of HCV-infected cells, JFH1-infected Huh7.5 cells were cocultured with LX2 cells, which are an HSC line generated by spontaneous immortalization in low-serum conditions (15). The expression of MIP-1β mRNA was then determined by qRT-PCR. Compared to the level in uninfected Huh7.5 cells, HCV infection induced a low level of MIP-1β expression (Fig. 1A, Huh7.5/JFH1). Moreover, MIP-1β expression

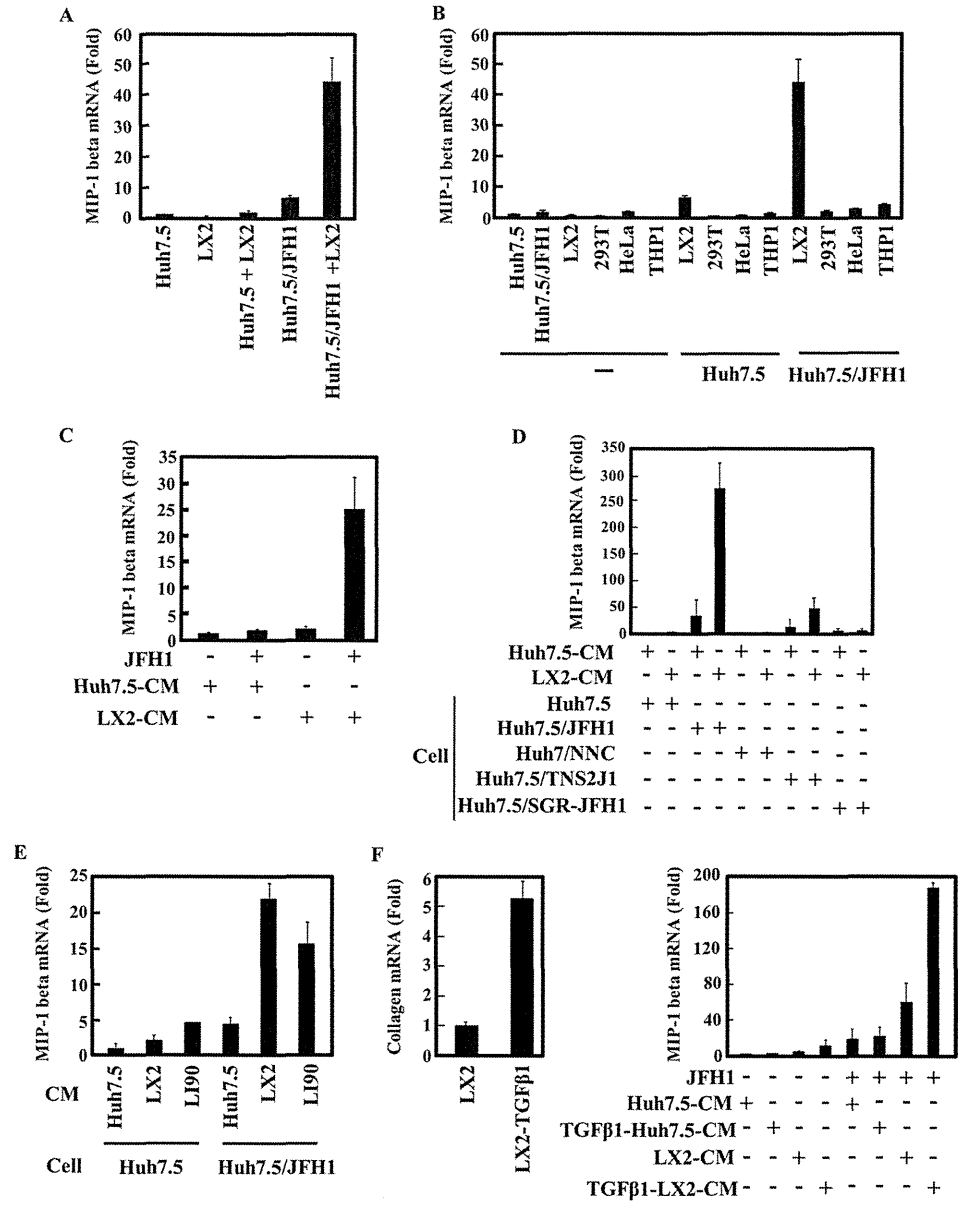

FIG 1 Conditioned medium from LX2 induces MIP-1β expression in JFH1-infected Huh7.5 cells. (A) Huh7.5 cells (1×10^5 cells) and JFH1-infected Huh7.5 (Huh7.5/JFH1) cells (1×10^5 cells) were cultured alone or in the presence of LX2 cells (1×10^5 cells) for 24 h. The level of MIP-1β was measured by qRT-PCR. Quantitative analysis of the PCR data was performed using the $2^{-\Delta\Delta CT}$ method, and glyceraldehyde-3-phosphate dehydrogenase (GAPDH) C_T values were used for normalization. The fold changes are relative to values for Huh7.5 cells. (B) Huh7.5 cells and JFH1-infected Huh7.5 cells (Huh7.5/JFH1) were cultured alone or in the presence of LX2, 293T, HeLa, or THP-1 cells for 24 h. The expression level of MIP-1β was measured by qRT-PCR as described for panel A. (C) Huh7.5 cells and JFH1-infected Huh7.5 cells were treated with conditioned medium from Huh7.5 (Huh7.5 CM) or LX2 (LX2 CM) cells for 24 h. The expression level of MIP-1β was measured by qRT-PCR as described for panel A. (D) Huh7.5, JFH1-infected Huh7.5 (Huh7.5/JFH1), Huh7/NNC, Huh7.5/TNS2J1, and Huh7.5/SGR-JFH1 cells were treated with CM from Huh7.5 or LX2 cells for 24 h. The expression level of MIP-1β was measured by qRT-PCR as described for panel A. (E) Huh7.5 and JFH1-infected Huh7.5 (Huh7.5/JFH1) cells were treated with Huh7.5 CM, LX2 CM, or LI90 CM for 24 h. The expression level of MIP-1β was measured by qRT-PCR as described for panel A. (F) LX2 cells were treated with 2.5 ng/ml TGF-β1 for 24 h, and then the level of collagen mRNA in these cells was determined by qRT-PCR (left). Huh7.5 or JFH1-infected Huh7.5 cells were treated with LX2 CM or TGF-β1-stimulated LX2 CM for 24 h. The expression level of MIP-1β was measured by qRT-PCR as described for panel A (right). The results are representative of three independent experiments, and the error bars represent the standard deviation of the means.

was significantly enhanced in JFH1-infected Huh7.5 cells after they were cocultured with LX2 cells (Fig. 1A, Huh7.5/JFH1+LX2). Importantly, MIP-1β expression was undetectable or very low in LX2 cells alone or in uninfected Huh7.5 cells cocultured with LX2 (Fig. 1A, LX2 and Huh7.5+LX2). Interestingly, increased MIP-1β expression in JFH1-infected Huh7.5 cells was specifically induced by cocultivation with LX2 cells. Cocultivation with other cell lines, such as 293T, HeLa, and THP-1, had no effect on MIP-1β expression in JFH1-infected Huh7.5 cells (Fig. 1B). These results suggest that Huh7.5 cells produce MIP-1β in re-

sponse to HCV infection and that LX2 cells increase MIP-1β expression in HCV-infected Huh7.5 cells.

We next determined whether MIP-1β induction by LX2 cells in HCV-infected cells was mediated by a secreted soluble factor(s). Huh7.5 and JFH1-infected Huh7.5 cells were treated with conditioned medium (CM) from Huh7.5 or LX2 cells (Fig. 1C). As expected, Huh7.5 cells had no response to Huh7.5 CM or LX2 CM. However, we observed that LX2 CM, but not Huh7.5 CM, stimulated MIP-1β expression in JFH1-infected Huh7.5 cells. These results indicated that LX2 cells secrete a factor that stimulates MIP-1β expression.

To address whether MIP-1β stimulation after culturing with LX2 CM is dependent on HCV genotype or on the maintenance of the HCV replicon in cells, we used Huh7.5 cells that carry different types of the HCV genome. Huh7/NNC cells are Huh7 cells that contain the noninfectious full HCV genotype 1b, Huh7.5/SGR-JFH1 cells contain the subgenome replicon of JFH1, and Huh7.5/TNS2J1 cells have the infectious chimeric HCV genome, which consists of an HCV-1b-derived sequence in the structural-protein-coding region and a JFH-derived sequence in nonstructural-protein-coding region (Fig. 1D). In Huh7.5/TNS2J1 cells, MIP-1β expression was significantly induced by LX2 CM (47-fold), though there was a lower level of expression than what was observed in JFH1-infected cells (272-fold). By contrast, NNC and SGR-JFH1 had no effect on MIP-1β expression. These results demonstrate that LX2 CM-induced stimulation of MIP-1β expression may require a productive HCV infection (see also Fig. 6).

Because LX2 cells are a human hepatic stellate cell line that was established by immortalization, we confirmed our findings by using another human hepatic stellate cell line, LI90, which was derived from a human mesenchymal liver tumor (16). When uninfected or JFH1-infected Huh7.5 cells were treated with LI90 CM, MIP-1β expression was increased only in the JFH1-infected Huh7.5 cells. These results are similar to those found after addition of LX2 CM to JFH1-infected Huh7.5 cells (Fig. 1E).

Activated hepatic stellate cells play a critical role in inflammation, yet the functional impact they have on hepatocytes has not yet been determined. Therefore, we evaluated whether the activation of LX2 cells affects the expression of MIP-1β in JFH1-infected Huh7.5 cells. LX2 cells were treated with TGF-β1, and the mRNA expression of the collagen gene, a marker of HSC activation, was measured (Fig. 1F, left). LX2 CM from activated cells significantly enhanced MIP-1β expression in JFH1-infected Huh7.5 cells but not in uninfected Huh7.5 cells, compared to the increase with nonactivated LX2 CM (Fig. 1F, right). In parallel experiments, TGF-β1-treated Huh7.5 CM did not affect MIP-1β expression in Huh7.5 or JFH1-infected Huh7.5 cells.

The supernatant from JFH1-infected Huh7.5 cells cultured with LX2 CM induces migration of NP-2-CCR5 cells. MIP-1β is a physiological ligand for the CCR5 receptor. To test whether MIP-1β produced by HCV-infected hepatocytes that have been cultured with LX2 CM has this activity, we performed a chemotactic assay using NP-2-CCR5 cells, a human glioma-derived cell line expressing CCR5 on its cell surface (Fig. 2). The treatment of NP-2-CCR5 cells with supernatant from LX2 CM-stimulated JFH1-infected Huh7.5 cells increased their migration by 2-fold compared to treatment with supernatant from uninfected Huh7.5 cells treated with LX2 CM. This increase in NP-2-CCR5 cell migration was blocked with maraviroc (a CCR5 antagonist) treatment. These results indicated that LX2 CM induces secretion of a physiologically functional MIP-1β by JFH1-infected Huh7.5 cells.

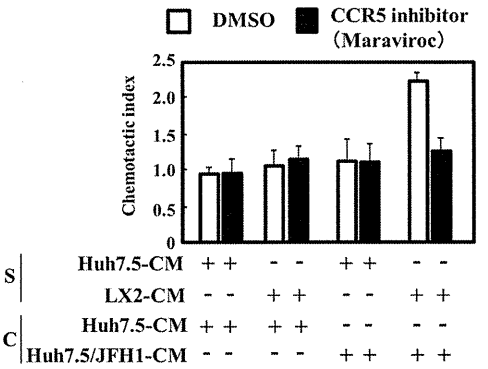

FIG 2 Conditioned medium from JFH1-infected Huh7.5 cells treated with LX2-conditioned medium induces chemotaxis of NP-2-CCR5 cells. Huh7.5 CM or LX2 CM was concentrated 60-fold using a 100,000-molecular-weight-cutoff membrane filter. Huh7.5 and Huh7.5/JFH1 cells were treated with each concentrated medium (S). After 24 h of treatment, the medium was changed to serum free DMEM for 24 h. The chemotactic activity of each conditioned medium (C) was determined by using 5 nM maraviroc (CCR5 inhibitor) and NP-2-CCR5 cells, as described in Materials and Methods. The results are representative of three independent experiments, and the error bars represent the standard deviations of the means. DMSO, dimethyl sulfoxide.

Identification of the factor in LX2 CM responsible for MIP-1β stimulation. We first fractionated culture medium of Huh7.5 or LX2 cells using a membrane filter which cut off the 100-kDa-molecular-mass marker protein and then collected the trapped and flowthrough fractions. As expected, MIP-1β expression in uninfected Huh7.5 or JFH1-infected Huh7.5 cells did not increase after treatment with the trap or the flowthrough fraction of the Huh7.5 CM (Fig. 3A). By contrast, the trap fraction of LX2 CM enhanced MIP-1β expression in JFH1-infected Huh7.5 cells, suggesting that the stimulator in the LX2 CM was enriched in the 100-kDa-molecular-mass-cutoff filter. To further analyze the trap fraction of LX2 CM, we created a cytokine antibody array (Fig. 3B). By analyzing 507 cytokines and chemokines in the array, we found four candidates (TSG-14, monocyte chemoattractant protein 2 [MCP-2], MCP-3, and IL-1α), which were more concentrated by the 100-kDa-molecular-mass-cutoff filter than by the flowthrough fraction of LX2 CM (Fig. 3B, compare 100K-Flow through to 100K-Trap). We tested the effects of these candidates on stimulation of MIP-1β expression (Fig. 4A). Although recombinant TSG-14, MCP-2, or MCP-3 did not stimulate MIP-1β expression in Huh7.5 cells or JFH1-infected cells, recombinant IL-1α induced MIP-1β expression in only JFH1-infected Huh7.5 cells. This effect was dose dependent (Fig. 4B). To evaluate whether IL-1α is required for MIP-1β stimulation in JFH1-infected Huh7.5 cells by LX2 CM, we used a neutralizing antibody against IL-1α and the IL-1 receptor antagonist. LX2 CM stimulated MIP-1β expression in JFH1-infected Huh7.5 cells, whereas anti-IL-1α and the IL-1 receptor antagonist (IL-1RA) blocked MIP-1β stimulation (Fig. 4C). Additionally, the neutralizing antibody against IL-1β had no effect (data not shown). It is not clear why IL-1α of about 30 kDa was concentrated into the trap fraction. However, it is likely that IL-1α is formed at a large mass with other proteins in the culture medium to be contained. Moreover, knockdown of IRAK1, which is essential for the downstream sig-

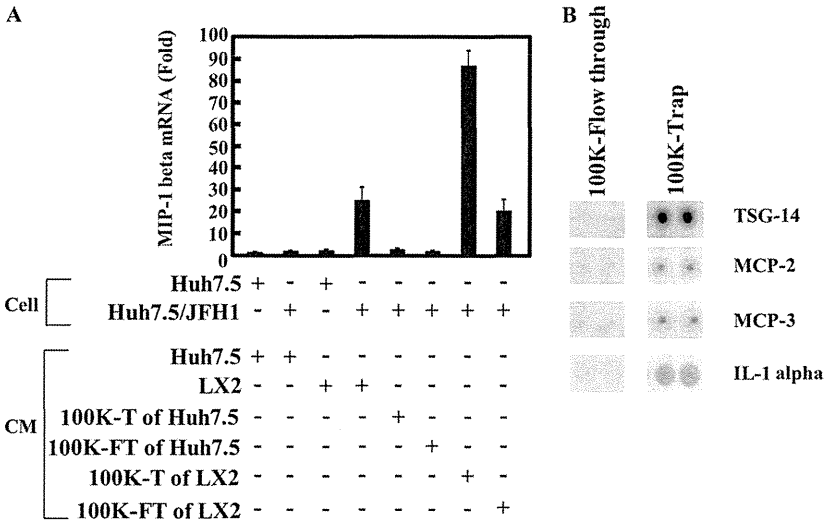

FIG 3 Identification of a factor(s) in the LX2 conditioned medium that is responsible for induction of MIP-1β expression. (A) Huh7.5 CM or LX2 CM was concentrated using a 100,000-molecular-weight-cutoff membrane filter. Huh7.5 and JFH1-infected Huh7.5 (Huh7.5/JFH1) cells were treated with each unconcentrated conditioned medium, with the flowthrough fraction (100K-FT), or with the trap fraction (100K-T). The MIP-1β expression level was analyzed by qRT-PCR as described for Fig. 1A. (B) LX2 CM was concentrated using a 100,000-molecular-weight-cutoff membrane filter. A cytokine antibody array (RayBiotech) was used for the simultaneous detection of 507 inflammatory factors. The antibody-coated membrane was incubated with the trap fraction (100K-Trap) or with the flowthrough fraction (100K-Flow through). Representative spots (TSG-14, MCP-1, MCP-3, and IL-1α) are shown.

nal of IL-1R, impaired the response to LX2 CM (Fig. 4D). These results suggest that IL-1α contributes to stimulation of MIP-1β expression by LX2 CM and that JFH1-infected Huh7.5 cells are highly sensitive to IL-1α. Furthermore, considering the molecular weight of IL-1α, it is possible that an unknown amount of IL-1α, undetectable by the cytokine antibody array, passed through the filter, which caused activation of MIP-1b by the 100,000-molecular-weight-cutoff flowthrough fraction. Alternatively, a factor(s) other than IL-1α in the 100,000-molecular-weight-cutoff flowthrough fraction might have been responsible for the activation.

The transcription factor C/EBPβ mediates LX2 CM-stimulated MIP-1β production. IL-1 is one of the most important proinflammatory cytokines and binds to the cell surface IL-1 type I receptor to activate downstream signaling pathways such as IKK–NF-κB, extracellular signal-regulated kinase (ERK), Jun N-terminal protein kinase (JNK), p38, and C/EBPβ. Moreover, the MIP-1β promoter contains a C/EBPβ motif located between bp −222 and −100, and the C/EBPβ promoter is required for a functional response to IL-1β in human chondrocytes (17). To evaluate whether LX2 CM-stimulated MIP-1β expression involves C/EBPβ stimulation, the level of C/EBPβ mRNA was measured in uninfected and HCV-infected cells. C/EBPβ expression was higher in Huh7.5/JFH1 and Huh7.5/TNS2J1 cells than in Huh7.5, Huh7/NNC, and Huh7.5/SGR-JFH1 cells (Fig. 5A). This result correlates with MIP-1β stimulation shown in Fig. 1D. Additionally, LX2 CM induced low levels of C/EBPβ expression in Huh7.5/JFH1 and Huh7.5/TNS2J1 cells; induction was likely caused by IL-1α (Fig. 5A). To further confirm that the enhancement of MIP-1β expression is mediated by C/EBPβ, we performed experiments where uninfected or JFH1-infected Huh7.5 cells were transduced with either a control or a C/EBPβ-specific siRNA and then treated with Huh7.5 CM or LX2 CM. Quantitative RT-PCR analysis demonstrated that the siRNAs targeting C/EBPβ significantly suppressed endogenous C/EBPβ expression (Fig. 5B). Depletion of C/EBPβ significantly reduced the MIP-1β expression stimulated by LX2 CM in JFH1-infected Huh7.5 cells. Residual stimulation of MIP-1β seems to be attributable to imperfect knockdown of C/EBPβ (70 to 80%). However, currently we cannot rule out the possibility of the involvement of other transcription factor(s) in the activation of MIP-1β expression. Furthermore, cytokines (IL-6, IL-8, CXCL2, CXCL1, MIP-1β, and MIP-1α) that were enhanced by C/EBPβ expression were upregulated by LX2 CM only in JFH1-infected Huh7.5 cells (Fig. 5D). There was no induction of C/EBPβ-independent cytokines (IL-7, CXCL6, CXCL5, IL-1α, and IL-1R) after the addition of LX2 CM. None of these cytokines were induced by LX2 CM in uninfected Huh7.5 cells. These data indicate that HCV stimulates C/EBPβ expression, which confers upon HCV-infected Huh7.5 cells the ability to produce proinflammatory cytokines in response to LX2 CM.

Early steps of the HCV life cycle trigger MIP-1β stimulation by LX2 CM. We observed that Huh7.5/TNS2J1 and Huh7.5/JFH1 cells, but not Huh7/NNC or Huh7.5/SGR-JFH1 cells, could respond to LX2 CM (Fig. 1D), suggesting that the production of infectious HCV is required for MIP-1β induction. However, it remains to be determined whether infectious HCV particles actually induce MIP-1β expression in the presence of LX2 CM. To address this question, we used JFH1-CL3B, which is a virus that is defective in the production of virus particles because of mutations in domain III of NS5A; however, the self-replication ability of its genome is normal (18). As shown in Fig. 6A, JFH1-CL3B genome-bearing Huh7.5 cells responded to neither Huh7.5 CM nor LX2 CM. These data suggest that productive infection of HCV is an essential event for MIP-1β induction. To characterize the mechanism that mediates LX2 CM-stimulated MIP-1β induction in HCV-infected cells, we studied the temporal kinetics of MIP-1β expression. In JFH1-infected Huh7.5 cells, MIP-1β expression did not increase in the first 2 h after infection but it started to increase after 4 h in the presence of LX2 CM (Fig. 6B). Furthermore,

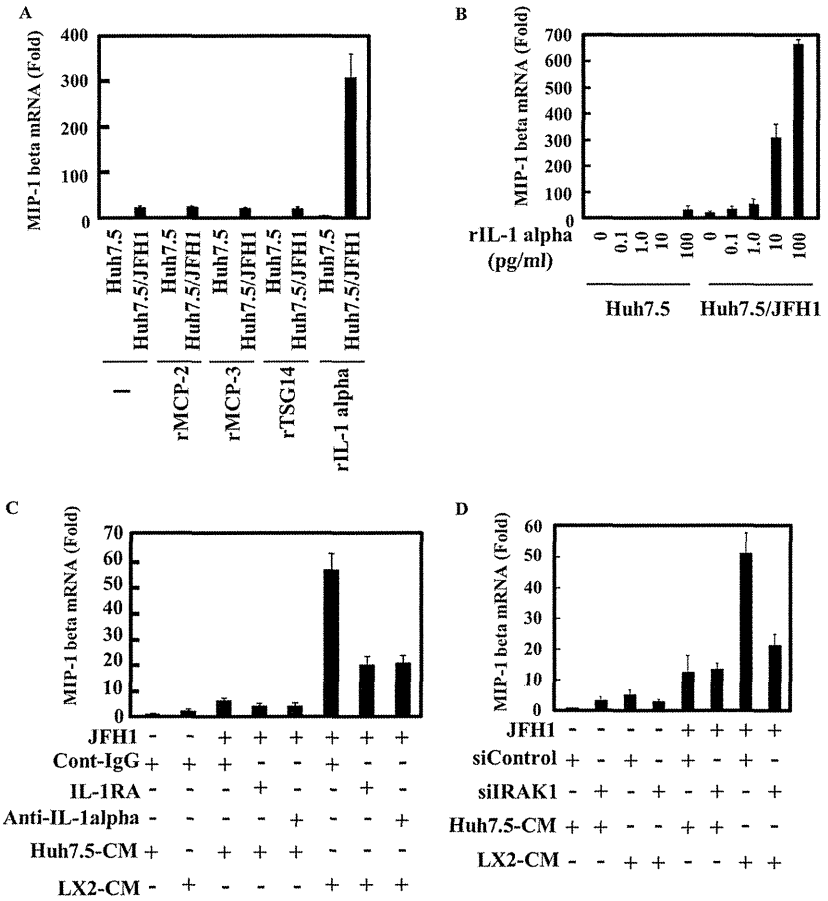

FIG 4 IL-1α induces MIP-1β expression in JFH1-infected Huh7.5 cells. (A) Huh7.5 and JFH1-infected Huh7.5 (Huh7.5/JFH1) cells were treated with recombinant MCP-2 (10 ng/ml), recombinant MCP-3 (rMCB-3; 10 ng/ml), recombinant TSG14 (10 ng/ml), or recombinant IL-1α (10 pg/ml) for 24 h. The level of MIP-1β expression was analyzed by qRT-PCR as described for Fig. 1A. (B) Huh7.5 and JFH1-infected Huh7.5 (Huh7.5/JFH1) cells were treated with various amounts of recombinant IL-1α (0, 0.1, 1.0, 10, or 100 pg/ml) for 24 h. The level of MIP-1β expression was analyzed by qRT-PCR as described for Fig. 1A. (C) JFH1-infected Huh7.5 cells were treated with Huh7.5 CM or LX2 CM along with an isotype control (0.2 μg/ml), anti-IL-1α (0.2 μg/ml), or IL-1RA (100 μg/ml) for 24 h. The level of MIP-1β expression was analyzed by qRT-PCR as described for Fig. 1A. (D) Huh7.5 and Huh7.5/JFH1 cells were transfected with 50 nM control siRNA (siControl) or 50 nM IRAK1 siRNA (siIRAK1). At 48 h after transfection, cells were treated with Huh7.5 CM or LX2 CM. The level of MIP-1β expression was analyzed by qRT-PCR as described for Fig. 1A. The results are representative of three independent experiments, and the error bars represent the standard deviations of the means.

MIP-1β induction in Huh7.5/JFH1 cells that were cultured in the presence of LX2 CM was suppressed by pretreatment of the cells with a neutralizing antibody against anti-CD81. To further address whether MIP-1β induction by LX2 CM in Huh7.5/JFH1 cells is due to the binding of HCV E1/E2 to the receptor, JFH1-infected cells were UV irradiated and used to infect Huh7.5 cells. Huh7.5 cells infected with UV-irradiated JFH1 did not show MIP-1β induction stimulated by LX2 CM (Fig. 6D). In addition, ectopic expression of HCV proteins in Huh7.5 cells did not respond to the LX2 CM (Fig. 6E). These results suggest that MIP-1β expression is required for HCV infection at postentry.

DISCUSSION

HCV-specific CTLs are concentrated within the liver during chronic infection, and they may control viral replication and contribute to progressive liver disease (19). Recruitment of T cells to the liver is required for the expression of CCR5 on activated T cells (20). Intrahepatic expression of the ligands for CCR5 (RANTES, MIP-1β, and MIP-1α) is elevated in HCV patients, and these chemokines have been linked to a high degree of liver inflammation (21). However, the mechanism mediating the stimulation of these cytokines is unclear. In this study, we demonstrated that cross talk between HCV-infected hepatocytes and human stellate cells (HSCs) induced inflammatory cytokines and chemokines. Importantly, uninfected hepatocytes are tolerant of HSC stimulation. Of note, HCV has no direct effect on LX2 cells with regard to MIP-1β stimulation because MIP-1β expression in Huh7.5/JFH1 cells was induced by treatment with CM from JFH1-treated LX2 cells as well as LX2 CM.

We identified IL-1α as an inducer of cytokines and chemokines in HCV-infected hepatocytes. These cells are highly sensitive to IL-1α (Fig. 4). Previous reports have indicated that the HCV core and NS3 proteins, which induced IL-1 receptor-associated kinase (IRAK) activity, triggered inflammatory cell activation through TLR-2 (22). IRAK activation by HCV infection may contribute to the induction of cytokines and chemokines by HSCs. We addressed this point and found that knockdown of IRAK1 in HCV-

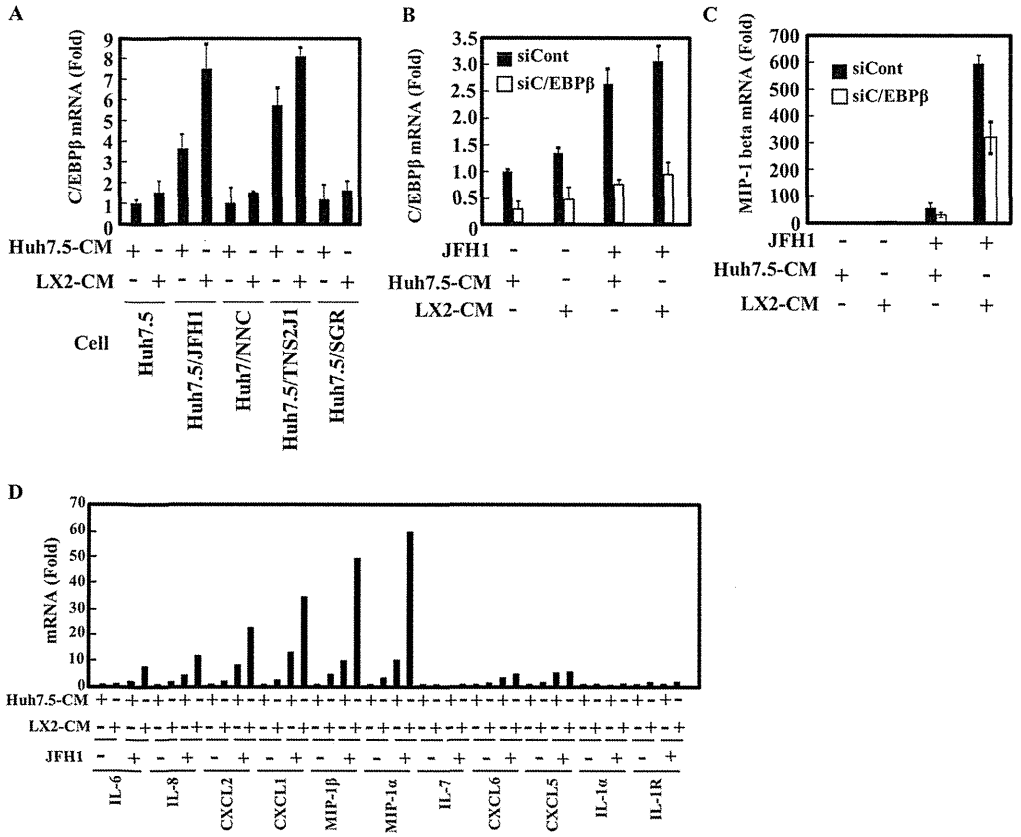

FIG 5 Conditioned medium from LX2 induces C/EBPβ-mediated proinflammatory gene expression in JFH1-infected Huh7.5 cells. (A) The indicated cells were treated with Huh7.5 CM or LX2 CM for 24 h. The level of C/EBPβ expression was analyzed by qRT-PCR as described for Fig. 1A. (B and C) Huh7.5 cells and JFH1-infected Huh7.5 cells were transfected with 50 nM control siRNA or siC/EBPβ. After 24 h of transfection, the cells were treated with Huh7.5 CM or LX2 CM for 24 h. The levels of C/EBPβ (B) and MIP-1β (C) expression were analyzed by qRT-PCR as described for Fig. 1A. (D) Huh7.5 cells and JFH1-infected Huh7.5 cells were treated with Huh7.5 CM or LX2 CM for 24 h. The levels of the indicated cytokines and chemokines were measured by qRT-PCR, as described for Fig. 1A. The results are representative of three independent experiments.

infected hepatocytes indicated that the response to HSC CM was impaired (Fig. 4D). By contrast, another group reported that HCV NS5A inhibits recruitment of IRAK to MyD88, resulting in suppression of the TLR signaling pathways in macrophage cell lines that stably expressed HCV NS5A (23). Currently, there is no evidence to suggest that HCV infects macrophages or that macrophages uptake functional NS5A to modulate TLR signaling. These conflicting results may be explained by the differences in cell types.

Our results suggest that IL-1α produced from hepatic stellate cells contributes to the inflammation by HCV infection *in vivo*. Another report shows augmented expression of IL-1α, tumor necrosis factor alpha (TNF-α), and IL-2 in HCV-infected patients compared to controls (24). Further, IL-1α plays roles in the liver to induce the acute-phase response of inflammation and autoactivation of Kupffer cells (25). Brain tissue from HCV patients, which is positive for HCV RNA and virus proteins, showed a significantly higher level of IL-1α than HCV-negative controls. Higher levels of proinflammatory cytokines such as IL-1α, IL-1β, TNF-α, IL-12, and IL-18 correlate with neurocognitive dysfunction among HCV patients. These results suggest that IL-1α is an important factor of HCV-related inflammation (26).

The relative importance of C/EBPβ in the stimulation of IL-1-inducible genes, such as the MIP-1α, MIP-1β, and IL-6 genes, is still not fully understood. Our results indicate that HCV-infected cells, which exhibited a 3- to 5-fold enhancement of C/EBPβ mRNA expression compared to uninfected cells (Fig. 5A), responded to IL-1α for the induction of MIP-1β mRNA synthesis. MIP-1β expression required the presence of C/EBPβ because knockdown of C/EBPβ significantly decreased LX2 CM-induced MIP-1β expression (Fig. 5C). To further address the relationship between C/EBPβ and MIP-1β, we analyzed the levels of C/EBPβ and MIP-1β mRNAs in uninfected Huh7.5 and Huh7.5/JFH1 cells in the presence of IL-1α (1 to 100 pg/ml) (data not shown). Compared with Huh7.5 cells, C/EBPβ expression was modestly induced in Huh7.5/JFH1 cells (about 4-fold) in the presence of 100 pg/ml IL-1α. By contrast, MIP-1β expression in Huh7.5/JFH1 cells at this dose of IL-1α was strongly induced (300-fold). These results indicate that IL-1α-induced MIP-1β mRNA induction in Huh7.5/JFH1 cells cannot be fully explained by the slight increase of C/EBPβ mRNA expression. It is known that C/EBPβ is modified posttranslationally (27, 28). C/EBPβ is phosphorylated by the Ras/mitogen-activated protein kinase (Ras/MAPK) pathway (29, 30), and a Ca^{2+}/calmodulin-dependent protein kinase (31) or ERK1/ERK2 stimulates the transactivation potential of C/EBPβ (32). C/EBPβ in HCV-infected cells may also be activated by a

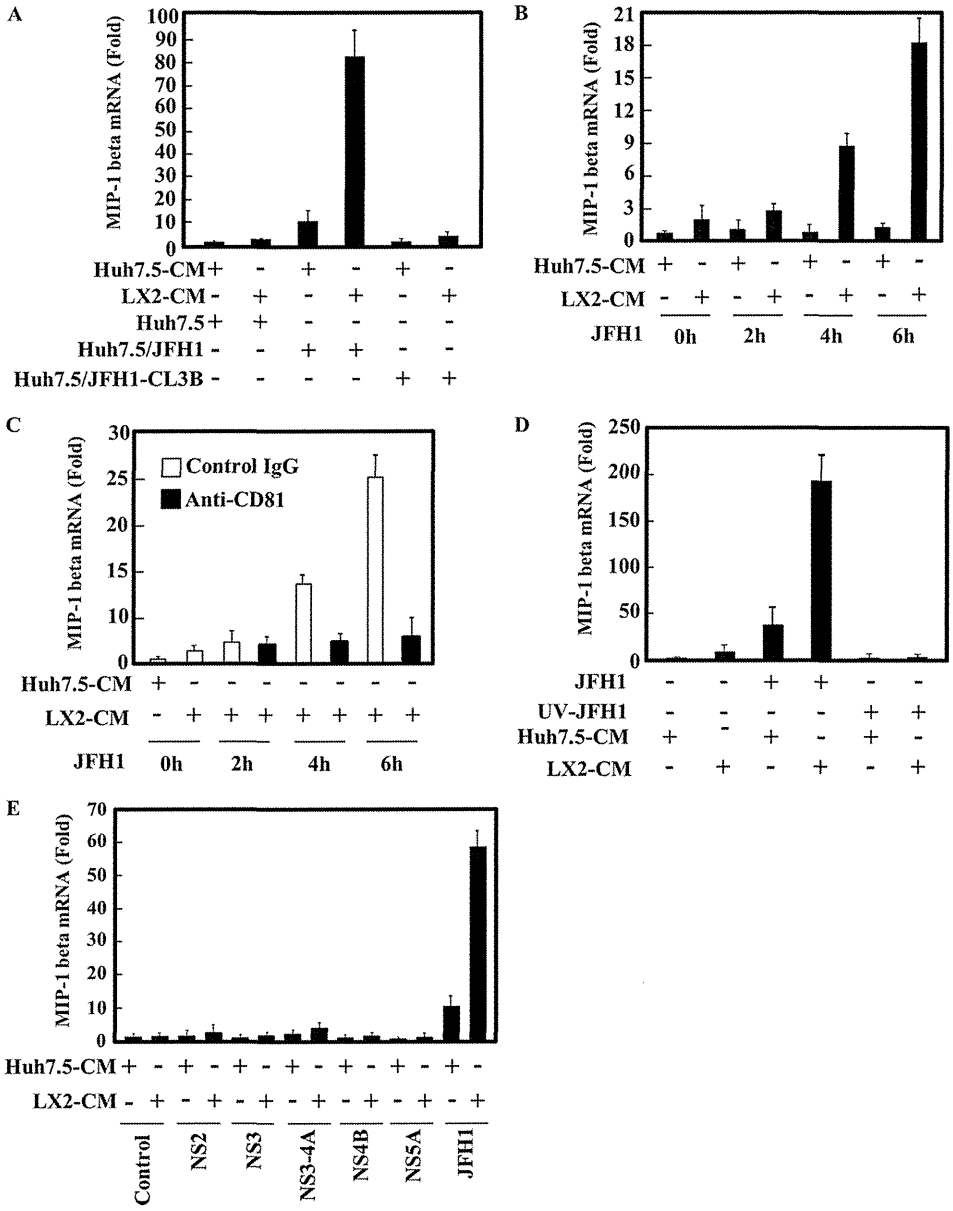

FIG 6 HCV entry is required for induction of MIP-1β expression by LX2 CM. (A) Huh7.5, JFH1-infected Huh7.5 (Huh7.5/JFH1), and JFH1-CL3B-infected Huh7.5 (Huh7.5/JFH1-CL3B) cells were treated with Huh7.5 CM or LX2 CM for 24 h. The level of MIP-1β expression was analyzed by qRT-PCR as described for Fig. 1A. (B) Huh7.5 cells were treated with Huh7.5 CM or LX2 CM. After 24 h of treatment, cells were infected with JFH1 for 2, 4, or 6 h. The level of MIP-1β expression was analyzed by qRT-PCR as described for Fig. 1A. (C) Huh7.5 cells were treated with Huh7.5 CM or LX2 CM in the presence of an isotype control IgG or anti-CD81 antibody (1 μg/ml). After 24 h of treatment, the cells were infected with JFH1 in the presence of an isotype control IgG or anti-CD81 antibody (1 μg/ml) for 2, 4, or 6 h. The level of MIP-1β expression was analyzed by qRT-PCR as described for Fig. 1A. (D) HCV JFH1 was UV irradiated and used to infect Huh7.5 cells. At 24 h after infection, cells were treated with Huh7.5 CM or LX2 CM. The level of MIP-1β expression was analyzed by qRT-PCR as described for Fig. 1A. (E) Huh7.5 cells expressing the indicated HCV proteins were treated with Huh7.5 CM or LX2 CM for 24 h. The levels of MIP-1β expression were analyzed by qRT-PCR as described for Fig. 1A. The results are representative of three independent experiments, and the error bars represent the standard deviations of the means.

posttranslational modification in response to IL-1 treatment. It is possible that activation of the MAPK (33) and ERK pathways (34) by HCV infection induces phosphorylation of C/EBPβ, leading to a highly sensitive IL-1 response. Further studies will be required to clarify the details of how HCV modulates increased MIP1-β production through both the C/EBPβ and IL-1 receptor signaling pathways.

This study revealed that induction of inflammatory cytokines and chemokines by cross talk between HSCs and HCV-infected hepatocytes primarily involves the activation of C/EBPβ-dependent gene transcription, such as transcription of the IL-6, IL-8, CXCL-1, and MIP-1β genes (Fig. 5). A recent study demonstrated that the HCV NS5A protein induces C/EBPβ expression (35). However, treatment of Huh7.5 cells that expressed NS5A with HCS

CM did not induce MIP-1β expression significantly (Fig. 6E). We also observed only a marginal increase in MIP-1β mRNA level by solitary expression of each HCV protein in Huh7.5 cells by addition of LX2 CM (Fig. 6E).

Moreover, previous reports have suggested that ER stress, which is induced by HCV infection, leads to the generation of mature sterol regulatory element-binding protein 1 (SREBP-1) (36, 37) and that the mature SREBP-1c can bind to the C/EBPβ promoter (36, 38), leading to induction of C/EBPβ. Additionally, SREBP-1c promoter activity was upregulated in core-transgenic mice in a PA28γ-dependent manner (39). Indeed, we observed that endoplasmic reticulum (ER) stress-related genes and SREBP-1c expression were enhanced by HCV infection. However, induction of SREBP-1c is not involved in this process because HCV-infected cells that had SREBP-1c knocked down could still respond to HSC CM (data not shown).

Chronic inflammation is triggered by many events that also can increase the risk of developing cancer. For example, *Helicobacter pylori* is associated with gastric cancer, and inflammatory bowel disease is associated with colon cancer. In particular, IL-6 is one of the clinical targets for cancer-related inflammation (2). The level of IL-6 expression correlates with a rapid progression from hepatitis to hepatocellular carcinomas (40). The Ras and Jak/Stat pathway, which is downstream of the IL-6 receptor, is activated in hepatocellular carcinomas that have a poor prognosis (41). Additionally, IL-8 is a proinflammatory cytokine that specifically attracts and activates human neutrophils. In HCV patients, pegylated IFN-α-2a (PEG-IFN-α-2a) and ribavirin therapy decreased the neutrophil count in virologic responders compared to nonresponders (42). Enhancement of expression of these cytokines as well as MIP-1β, described here, suggests that the cross talk between HCV-infected hepatocytes and HSCs polarizes the cytokine profile toward a Th2-type immune response.

In conclusion, we have demonstrated that the cross talk between HSCs and HCV-infected hepatocytes results in the induction of inflammatory cytokines and chemokines, which promote the migration of CCR5-expressing cells in *in vitro* experiments. These results suggest that the induction of inflammatory cytokines and chemokines by HCV infection may recruit inflammatory cells such as cytotoxic T lymphocytes (CTL) and neutrophils to the liver, which induces liver cell injury leading to chronic hepatitis.

ACKNOWLEDGMENTS

We are grateful to H. Hoshino at Gunma University, C. Rice at The Rockefeller University, S. Friedman at Mount Sinai School of Medicine, and T. Wakita at the National Institute of Infectious Diseases for their contributions of research materials and to H. Yamamoto and R. Shiina for their technical assistance.

This work was partly supported by Grants-in-Aid for Scientific Research from the Ministry of Education, Culture, Sports, Science and Technology (MEXT), by the MEXT-Supported Program for the Strategic Research Foundation at Private Universities, and by grants-in-aid for research on hepatitis from the Ministry of Health, Labor, and Welfare of Japan.

REFERENCES

1. **Bartosch B, Thimme R, Blum HE, Zoulim F.** 2009. Hepatitis C virus-induced hepatocarcinogenesis. J. Hepatol. 51:810–820.
2. **Bowen DG, Walker CM.** 2005. Adaptive immune responses in acute and chronic hepatitis C virus infection. Nature 436:946–952.
3. **Liaw YF, Lee CS, Tsai SL, Liaw BW, Chen TC, Sheen IS, Chu CM.** 1995. T-cell-mediated autologous hepatocytotoxicity in patients with chronic hepatitis C virus infection. Hepatology 22:1368–1373.
4. **Shields PL, Morland CM, Salmon M, Qin S, Hubscher SG, Adams DH.** 1999. Chemokine and chemokine receptor interactions provide a mechanism for selective T cell recruitment to specific liver compartments within hepatitis C-infected liver. J. Immunol. 163:6236–6243.
5. **Harvey CE, Post JJ, Palladinetti P, Freeman AJ, Ffrench RA, Kumar RK, Marinos G, Lloyd AR.** 2003. Expression of the chemokine IP-10 (CXCL10) by hepatocytes in chronic hepatitis C virus infection correlates with histological severity and lobular inflammation. J. Leukoc. Biol. 74: 360–369.
6. **Napoli J, Bishop GA, McGuinness PH, Painter DM, McCaughan GW.** 1996. Progressive liver injury in chronic hepatitis C infection correlates with increased intrahepatic expression of Th1-associated cytokines. Hepatology 24:759–765.
7. **Basu A, Meyer K, Lai KK, Saito K, Di Bisceglie AM, Grosso LE, Ray RB, Ray R.** 2006. Microarray analyses and molecular profiling of Stat3 signaling pathway induced by hepatitis C virus core protein in human hepatocytes. Virology 349:347–358.
8. **Li K, Li NL, Wei D, Pfeffer SR, Fan M, Pfeffer LM.** 2012. Activation of chemokine and inflammatory cytokine response in hepatitis C virus-infected hepatocytes depends on Toll-like receptor 3 sensing of hepatitis C virus double-stranded RNA intermediates. Hepatology 55:666–675.
9. **Wagoner J, Austin M, Green J, Imaizumi T, Casola A, Brasier A, Khabar KS, Wakita T, Gale M, Jr, Polyak SJ.** 2007. Regulation of CXCL-8 (interleukin-8) induction by double-stranded RNA signaling pathways during hepatitis C virus infection. J. Virol. 81:309–318.
10. **Yu GY, He G, Li CY, Tang M, Grivennikov S, Tsai WT, Wu MS, Hsu CW, Tsai Y, Wang LH, Karin M.** 2012. Hepatic expression of HCV RNA-dependent RNA polymerase triggers innate immune signaling and cytokine production. Mol. Cell 48:313–321.
11. **Friedman SL.** 2008. Hepatic stellate cells: protean, multifunctional, and enigmatic cells of the liver. Physiol. Rev. 88:125–172.
12. **Friedman SL.** 2008. Mechanisms of hepatic fibrogenesis. Gastroenterology 134:1655–1669.
13. **Hernandez-Gea V, Friedman SL.** 2011. Pathogenesis of liver fibrosis. Annu. Rev. Pathol. 6:425–456.
14. **Coulouarn C, Corlu A, Glaise D, Guénon I, Thorgeirsson SS, Clément B.** 2012. Hepatocyte-stellate cell cross-talk in the liver engenders a permissive inflammatory microenvironment that drives progression in hepatocellular carcinoma. Cancer Res. 72:2533–2542.
15. **Xu L, Hui AY, Albanis E, Arthur MJ, O'Byrne SM, Blaner WS, Mukherjee P, Friedman SL, Eng FJ.** 2005. Human hepatic stellate cell lines, LX-1 and LX-2: new tools for analysis of hepatic fibrosis. Gut 54:142–151.
16. **Murakami K, Abe T, Miyazawa M, Yamaguchi M, Masuda T, Matsuura T, Nagamori S, Takeuchi K, Abe K, Kyogoku M.** 1995. Establishment of a new human cell line, LI90, exhibiting characteristics of hepatic Ito (fat-storing) cells. Lab. Invest. 72:731–739.
17. **Zhang Z, Bryan JL, DeLassus E, Chang LW, Liao W, Sandell LJ.** 2010. CCAAT/enhancer-binding protein β and NF-κB mediate high level expression of chemokine genes CCL3 and CCL4 by human chondrocytes in response to IL-1β. J. Biol. Chem. 285:33092–33103.
18. **Masaki T, Suzuki R, Murakami K, Aizaki H, Ishii K, Murayama A, Date T, Matsuura Y, Miyamura T, Wakita T, Suzuki T.** 2008. Interaction of hepatitis C virus nonstructural protein 5A with core protein is critical for the production of infectious virus particles. J. Virol. 82:7964–7976.
19. **Freeman AJ, Pan Y, Harvey CE, Post JJ, Law MG, White PA, Rawlinson WD, Lloyd AR, Marinos G, Ffrench RA.** 2003. The presence of an intrahepatic cytotoxic T lymphocyte response is associated with low viral load in patients with chronic hepatitis C virus infection. J. Hepatol. 38: 349–356.
20. **Zeremski M, Petrovic LM, Talal AH.** 2007. The role of chemokines as inflammatory mediators in chronic hepatitis C virus infection. J. Viral Hepat. 14:675–687.
21. **Wald O, Weiss ID, Galun E, Peled A.** 2007. Chemokines in hepatitis C virus infection: pathogenesis, prognosis and therapeutics. Cytokine 39: 50–62.
22. **Dolganiuc A, Oak S, Kodys K, Golenbock DT, Finberg RW, Kurt-Jones E, Szabo G.** 2004. Hepatitis C core and nonstructural 3 proteins trigger toll-like receptor 2-mediated pathways and inflammatory activation. Gastroenterology 127:1513–1524.
23. **Abe T, Kaname Y, Hamamoto I, Tsuda Y, Wen X, Taguwa S, Moriishi**

K, Takeuchi O, Kawai T, Kanto T, Hayashi N, Akira S, Matsuura Y. 2007. Hepatitis C virus nonstructural protein 5A modulates the toll-like receptor-MyD88-dependent signaling pathway in macrophage cell lines. J. Virol. 81:8953–8966.
24. Kasprzak A, Zabel M, Biczysko W, Wysocki J, Adamek A, Spachacz R, Surdyk-Zasada J. 2004. Expression of cytokines (TNF-alpha, IL-1alpha, and IL-2) in chronic hepatitis C: comparative hybridocytochemical and immunocytochemical study in children and adult patients. J. Histochem. Cytochem. 52:29–38.
25. Winwood PJ, Arthur MJ. 1993. Kupffer cells: their activation and role in animal models of liver injury and human liver disease. Semin. Liver Dis. 13:50–59.
26. Wilkinson J, Radkowski M, Eschbacher JM, Laskus T. 2010. Activation of brain macrophages/microglia cells in hepatitis C infection. Gut 59: 1394–1400.
27. Harrison JR, Kelly PL, Pilbeam CC. 2000. Involvement of CCAAT enhancer binding protein transcription factors in the regulation of prostaglandin G/H synthase 2 expression by interleukin-1 in osteoblastic MC3T3-E1 cells. J. Bone Miner. Res. 15:1138–1146.
28. Akira S, Isshiki H, Sugita T, Tanabe O, Kinoshita S, Nishio Y, Nakajima T, Hirano T, Kishimoto T. 1990. A nuclear factor for IL-6 expression (NF-IL6) is a member of a C/EBP family. EMBO. J. 9:1897–1906.
29. Nakajima T, Kinoshita S, Sasagawa T, Sasaki K, Naruto M, Kishimoto T, Akira S. 1993. Phosphorylation at threonine-235 by a ras-dependent mitogen-activated protein kinase cascade is essential for transcription factor NF-IL6. Proc. Natl. Acad. Sci. U. S. A. 90:2207–2211.
30. Zhu S, Yoon K, Sterneck E, Johnson PF, Smart RC. 2002. CCAAT/enhancer binding protein-beta is a mediator of keratinocyte survival and skin tumorigenesis involving oncogenic Ras signaling. Proc. Natl. Acad. Sci. U. S. A. 99:207–212.
31. Wegner M, Cao Z, Rosenfeld MG. 1992. Calcium-regulated phosphorylation within the leucine zipper of C/EBP beta. Science 256:370–373.
32. Giltiay NV, Karakashian AA, Alimov AP, Ligthle S, Nikolova-Karakashian MN. 2005. Ceramide- and ERK-dependent pathway for the activation of CCAAT/enhancer binding protein by interleukin-1beta in hepatocytes. J. Lipid Res. 46:2497–2505.
33. George A, Panda S, Kudmulwar D, Chhatbar SP, Nayak SC, Krishnan HH. 2012. Hepatitis C virus NS5A binds to the mRNA cap-binding eukaryotic translation initiation 4F (eIF4F) complex and up-regulates host translation initiation machinery through eIF4E-binding protein 1 inactivation. J. Biol. Chem. 287:5042–5058.
34. Zhao LJ, Wang L, Ren H, Cao J, Li L, Ke JS, Qi ZT. 2005. Hepatitis C virus E2 protein promotes human hepatoma cell proliferation through the MAPK/ERK signaling pathway via cellular receptors. Exp. Cell Res. 305: 23–32.
35. Qadri I, Choudhury M, Rahman SM, Knotts TA, Janssen RC, Schaack J, Iwahashi M, Puljak L, Simon FR, Kilic G, Fitz JG, Friedman JE. 2012. Increased phosphoenolpyruvate carboxykinase gene expression and steatosis during hepatitis C virus subgenome replication: role of nonstructural component 5A and CCAAT/enhancer-binding protein β. J. Biol. Chem. 287:37340–37351.
36. Lei X, Zhang S, Barbour SE, Bohrer A, Ford EL, Koizumi A, Papa FR, Ramanadham S. 2010. Spontaneous development of endoplasmic reticulum stress that can lead to diabetes mellitus is associated with higher calcium-independent phospholipase A2 expression: a role for regulation by SREBP-1. J. Biol. Chem. 285:6693–6705.
37. Joyce MA, Walters KA, Lamb SE, Yeh MM, Zhu LF, Kneteman N, Doyle JS, Katze MG, Tyrrell DL. 2009. HCV induces oxidative and ER stress, and sensitizes infected cells to apoptosis in SCID/Alb-uPA mice. PLoS Pathog. 5:e1000291. doi:10.1371/journal.ppat.1000291.
38. Le Lay S, Lefrère I, Trautwein C, Dugail I, Krief S. 2002. Insulin and sterol-regulatory element-binding protein-1c (SREBP-1C) regulation of gene expression in 3T3-L1 adipocytes. Identification of CCAAT/enhancer-binding protein beta as an SREBP-1C target. J. Biol. Chem. 277: 35625–35634.
39. Moriishi K, Mochizuki R, Moriya K, Miyamoto H, Mori Y, Abe T, Murata S, Tanaka K, Miyamura T, Suzuki T, Koike K, Matsuura Y. 2007. Critical role of PA28gamma in hepatitis C virus-associated steatogenesis and hepatocarcinogenesis. Proc. Natl. Acad. Sci. U. S. A. 104:1661–1666.
40. Wong VW, Yu J, Cheng AS, Wong GL, Chan HY, Chu ES, Ng EK, Chan FK, Sung JJ, Chan HL. 2009. High serum interleukin-6 level predicts future hepatocellular carcinoma development in patients with chronic hepatitis B. Int. J. Cancer 124:2766–2770.
41. Calvisi DF, Ladu S, Gorden A, Farina M, Conner EA, Lee JS, Factor VM, Thorgeirsson SS. 2006. Ubiquitous activation of Ras and Jak/Stat pathways in human HCC. Gastroenterology 130:1117–1128.
42. Chung RT, Poordad FF, Hassanein T, Zhou X, Lentz E, Prabhakar A, Di Bisceglie AM. 2010. Association of host pharmacodynamic effects with virologic response to pegylated interferon alfa-2a/ribavirin in chronic hepatitis C. Hepatology 52:1906–1914.